Joint Detection and Decoding for Polar-Coded IDMA-MIMO Systems

Weththasinghe Arachchige Rangana Kithmini

(169225V)

Degree of Master of Science

Department of Electronic and Telecommunication Engineering

University of Moratuwa
Moratuwa, Sri Lanka

April 2022

Abstract

The demand on data traffic and bandwidth requirements have continued to grow exponentially. Nevertheless, existing fourth generation (4G) networks are not capable of meeting those demands for high data rates and bandwidth requirements. Therefore, the fifth generation (5G) wireless access technology, which guarantees high spectral efficiency, low latency, and massive connectivity, was recently introduced. Non orthogonal multiple access (NOMA), which enables massive connectivity, was one of the key potential physical-layer technologies considered for 5G. Interleave division multiple access (IDMA) scheme is one of the promising NOMA schemes, with packet level interleavers to distinguish multiple access users. On the other hand, recently, polar codes have received increased attention as a capacity approaching code. Polar codes have already been adopted as the channel coding technique for the physical-layer control channel of 5G New Radio (NR) networks. In the literature, to date, there is only limited research on polar-coded IDMA systems. Multiple-Input Multiple Output (MIMO) enables the spatial degrees of freedom through use of multiple antennas at both the transmitter and the receiver. MIMO has been one of the key enabling technologies in recent standardized wireless communication systems including 3G HSPA and 4G LTE systems. The performance benefits of both IDMA and MIMO can be obtained by combining two technologies.

To this end, in this research study, an extension of conventional polar-coded IDMA to MIMO is considered for uplink communication. A polar-coded IDMA-MIMO uplink system model with QPSK modulation is proposed. An iterative receiver scheme is devised for polar-coded IDMA-MIMO systems. In the proposed receiver, likelihood messages are exchanged in each iteration between the soft multiuser MIMO detector and belief propagation (BP) algorithm-based decoder. The error performance of the proposed system is investigated using simulation for different system configurations. The simulation results confirm that polar coding offers significant performance improvement over the uncoded IDMA-MIMO system. Moreover, considerably improved error performance can be obtained by using the proposed iterative receiver scheme over single-pass multiuser MIMO detection and decoding. Further, higher the signal to noise ratio, the faster the convergence rate is.

Keywords:
5G, belief propagation (BP), interleave division multiple access (IDMA), joint detection and decoding (JDD), multiple input multiple output (MIMO), non-orthogonal multiple access (NOMA), polar codes (PC).

Declaration

I declare that this is my own work and this thesis does not incorporate without acknowledgement any material previously submitted for a Degree or Diploma in any other University or institute of higher learning and to the best of my knowledge and belief it does not contain any material previously published or written by another person except where the acknowledgement is made in the text.

Also, I hereby grant to University of Moratuwa the non-exclusive right to reproduce and distribute my thesis, in whole or in part in print, electronic or other medium. I retain the right to use this content in whole or part in future works (such as articles or books).

Signature | Date

The above candidate has carried out research for the Masters thesis under my supervision.

Signature of the supervisor | Date

Acknowledgement

This work was carried out during the years 2017-2021 at the Department of Electronic and Telecommunication Engineering, University of Moratuwa.

I owe my deepest gratitude to my supervisors Dr. Chandika Wawegedara his incredible guidance to successfully complete the research. I would like to thank the Senate Research Council, University of Moratuwa for supporting this work.

I would like to thank all the authors and owners of the materials that have been referred in this thesis and finally, I would like to thank all the people who supported to successfully complete the research.

Contents

List of Figures

List of Tables

List of Abbreviations

NOMA	Non Orthogonal Multiple Access
OMA	Orthogonal Multiple Access
BER	Bit Error Rate
BICM	Bit Interleaved Coded Modulation
BP	Belief Propagation
CDMA	Code Division Multiple Access
CRC-SCL	Cyclic Redundancy Check Aided SCL
eMMB	Enhanced Mobile Broadband
FDMA	Frequency Division Multiple Access
IDMA	Interleave Division Multiple Access
ITU-R	International Telecommunication Union Radiocommunication
JDD	Joint Detection and Decoding
JIDD	Joint Iterative Detection and decoding
LDPC	Low Density Parity Check
LDS-CDMA	Low-Density Spreading CDMA
LLR	Log Likelihood Ratio
MIMO	Multiple Input Multiple Output
MLCM	Multilevel Coded Modulation
MPA	Message Passing Algorithm

MUSA	Multiuser Shared Access
NLP	New Logistic Map
NR	New Radio
OFDMA	Orthogonal Frequency Division Multiple Access
PC	Polar Codes
PC-NOMA	Polar Coded Noma
PDMA	Pattern Division Multiple Access
PI	Prime Interleaver
PRE	Physical Resource Element
SCAN	Soft Cancellation
SCD	Successive Cancellation Decoding
SC-FDMA	Single Carrier FDMA
SCH	Successive Cancellation Heap
SCL	Successive Cancellation List
SCMA	Sparse Code Multiple Access
SDD	Separate Detection and Decoding
SIC	Successive Interference Cancellation
SINR	Signal to Interference Noise Ratio
TBI	Tree Based Interleaver
TDMA	Time Division Multiple Access
URLLC	Ultra-Reliable Low Latency Communications

Chapter 1

Introduction

1.1 Introduction

The fifth generation (5G) wireless communication networks are guaranteed to provide much higher spectral efficiency and data rates, with ultra-low latency and massive connectivity compared to the existing fourth generation (4G) networks as outlined by International Telecommunication Union Radiocommunication (ITU-R) sector [1]. The key radio access technologies for 5G include massive Multiple Input Multiple Output (MIMO), non-orthogonal multiple access (NOMA), millimeter-wave communication, small site networks, adaptive beamforming, and advanced channel coding schemes [2].

Conventional orthogonal multiple access (OMA) techniques: time division multiple access (TDMA), frequency division multiple access FDMA, code division multiple access (CDMA), single carrier FDMA (SC-FDMA), and orthogonal frequency division multiple access (OFDMA) are used so far in second, third, and fourth generation mobile communication systems. The basic idea of OMA is allocation of multiple users to orthogonal resources by reducing inter carrier interference. The use of orthogonality in resource allocation, underutilizes the limited licensed spectrum by limiting the number of simultaneous connections [3]. Hence, existing OMA technologies may not be able to cater for the massive connectivity requirements in 5G and beyond 5G networks. Therefore, in the literature various NOMA technologies have been proposed for 5G [3,4]. In NOMA technologies the number of carriers is increased using the property of non-orthogonality by intentionally introducing controllable interference among users allowing users to share the same resources [2].

NOMA schemes can be broadly categorized into two groups: power domain NOMA and code domain NOMA. The power domain NOMA scheme for downlink allocates different power levels for different users, according to their channel conditions, such that more transmission power for the users with poor channel conditions and vice versa [3]. To achieve the desired performance at the receiver, the channel gain difference among users should be adequate, which limits the effective number of multiple access users. In this scheme, the Successive Interference Cancellation (SIC) method was used at the receiver for detection. High receiver complexity, high energy consumption, and error propagation are the key drawbacks of the SIC approach. Therefore, in the literature Message Passing Algorithm (MPA) base receivers were proposed to reduce the receiver complexity [3]. The Belief Propagation (BP) decoding scheme is a MPA which iteratively updates soft messages between factor graph nodes [5].

Code domain NOMA includes Sparse Code Multiple Access (SCMA). In SCMA, different users are assigned to different codes and multiplex over time or frequency resources [2,3]. Another type of NOMA scheme is Pattern Division Multiple Access (PDMA) which uses multiple domain non-orthogonal patterns [3, 4]. Therefore, multiplexing can be achieved in either code domain, power domain or in spatial domain, or in any combination of them. Interleave Division Multiple Access (IDMA) uses packet level interleavers to distinguish users. In IDMA different interleavers are used for different users to provide adjacent packets approximately uncorrelated [6].

The comparison of different NOMA schemes was done based on system performance and computational complexity in [2, 3, 7]. SCMA and PDMA cause some performance losses due to codebook and pattern collisions respectively. According to the computational complexity analysis done in [3, 7], SCMA shows the highest computational complexity compared to the other NOMA schemes and IDMA shows the lowest computational complexity. Therefore, IDMA is a much preferred NOMA candidate for 5G and future networks. For IDMA, comparison of different types of interleaver designs, including random interleavers, power interleavers, and tree based interleavers, were presented in [8–10].

In wireless communications systems, channel coding techniques are used for detection and correction of bit errors that occurred in transmission due to noise, interference, and channel fading. Turbo codes and low density parity check (LDPC) codes are the most commonly used channel coding techniques in recent standard wireless communication systems [2]. Recently, polar codes have received tremendous attention. The concept of polar coding was first proposed by Arikan in 2009 [11]. LDPC codes and polar codes have been employed for the data channels and control channels of 5G 3GPP NR, respectively [1]. Data plane applications of polar codes on longer length codes are limited due to the design complexity of achieving low latency and high throughput [2].

Different NOMA schemes with different channel coding techniques were analyzed based on bit error rate (BER) performance and receiver complexity. It was shown that polar coded NOMA schemes have better bit error performance. Polar coded SCMA with successive cancellation decoding (SCD) outperforms turbo coded SCMA [12]. Polar coded PDMA with SCD outperforms turbo coded PDMA [12]. Moreover, polar coded SCMA with cyclic redundancy check aided SCL (CRC-SCL) decoding outperforms LDPC-SCMA, because LDPC codes have higher decoding complexity compared to polar codes. A separate detection and decoding (SDD) method is used in conventional polar coded NOMA schemes, where there are two factor graphs for detection and decoding [13]. The detection of received signal is first performed to generate likelihood messages of coded bits and then those likelihood messages are used in decoding. In the joint detection and decoding (JDD) approach, likelihood messages are exchanged between the detection and decoding graphs within the same iteration [13, 14]. This improves decoding because likelihood messages are updated by both graphs iteratively. This joint iterative processing is possible with the BP decoder because of its parallel nature of processing. Therefore, the BP polar decoder has become a preferable choice for high throughput applications [5].

1.2 Problem Statement

Higher coding gain, better reliability, and low decoder power consumption are some of the key advantages of polar codes compared to conventional coding schemes. Polar codes have been already adopted in 5G networks as the channel coding methods for the control channels. Channel coding techniques are used for detection and correction of bit errors that occurred in transmission due to noise, interference, and channel fading. Polar Coded NOMA (PC-NOMA) is one of the promising technologies to meet the requirements of 5G and beyond 5G networks. Improved performance can be obtained by using applications of polar codes with NOMA systems. IDMA uses packet level interleavers to distinguish users. IDMA shows the lowest computational complexity. Therefore, IDMA is a much preferred NOMA candidate for 5G and future networks. Research on polar coded NOMA has received relatively limited attention so far. Though there were some research studies on polar-coded NOMA, only a limited number of research attempts have focused on polar-coded IDMA systems. On the other hand, the performance benefits of both IDMA and MIMO can be obtained by combining two technologies. For example, we can obtain significant improvement in the attainable spectral efficiency through application IDMA in MIMO systems. Thus, it is important to extend conventional polar-coded IDMA to MIMO with multiple antennas employed at both the multiuser transmitters and basestation receiver. Moreover, improved error performance can be gained by using an advanced iterative receiver in polar-coded IDMA- MIMO systems.

1.3 Objectives and Scope

This research study focuses on application of polar codes in multiuser IDMA-MIMO systems for the uplink transmission. The key research objectives can be summarized as follows:

- To conduct literature reviews on polar codes, NOMA, and polar-coded NOMA schemes
- To propose a system model for multiuser IDMA-MIMO uplink transmission
- To develop an iterative receiver for polar-coded multiuser IDMA-MIMO uplink systems
- To investigate the error performance of the proposed receiver scheme under different system configurations and scenarios

The work of this research study can be considered as an extension to work of [15]. Polar encoding can be employed at the transmitter [15] instead of convolution coding. Further, QPSK modulation can be used instead of BPSK modulation. The key technical contributions can be summarized as follows.

- An IDMA-MIMO system model is proposed for polar-coded multiuser uplink transmission with spatial multiplexing and QPSK modulation.
- A soft-input soft-output multiuser MIMO detector is developed to soft detect QPSK modulated signals.
- An iterative receiver scheme, which consists of the soft-input soft-output multiuser MIMO detector and the BP algorithm-based polar detector is proposed.
- The performance of the proposed iterative receiver scheme is investigated for different system scenarios through simulation.

In the system model, the channel can be assumed to be a Rayleigh fading channel and each MIMO channel coefficient can be assumed to be time-invariant. The receiver proposed in [15] consists of soft multiuser detector, de-interleavers, interleavers and soft channel decoders, which can be improved by extending the soft multiuser MIMO detector for complex channels and employing a belief propagation decoding algorithm for polar decoder. Further, an iterative detection and decoding scheme can be employed at the receiver, allowing soft messages to exchange between modules within the same iteration.

1.4 Methodology

This section summarizes the research methodology.

- Identify core research papers on polar codes and IDMA. Identify research on different NOMA schemes and polar-coded NOMA schemes in the literature to conduct the literature review.
- Analyze different transceiver structures proposed in the literature to gain an understanding of the existing research and to identify inconsistencies in research. Compare and contrast those schemes based on the NOMA schemes used, decoding algorithms, BER performance and receiver complexity.
- Develop an IDMA-MIMO transmitter with polar code encoding and QPSK modulation.
- Develop a soft multiuser MIMO detector to perform muliuser detection and soft QPSK demodulation.
- Integrate the soft multiuser MIMO detector with soft BP algorithm-based polar decoders using deinterleavers, despreaders, spreaders and interleavers.
- Iteratively perform multiuser MIMO detection and BP polar decoding by exchanging soft messages between multiuser MIMO detector and BP polar decoder.
- Compare the BER performance of the proposed polar coded multiuser MIMO system with a uncoded multiuser MIMO system through simulation.
- Analyze the variation of the BER performance of the proposed iterative receiver with different system parameters including the number of detection and decoding iterations, number of multiple access users, number of transmit antennas, and spreading factor through simulation.

1.5 Notation

The notations and symbols used in this paper are given in Table 1.

1.6 Organization of the Thesis

The remainder of this thesis is organized as follows. Chapter 2 presents the literature survey and related work. It provides a comprehensive review of different NOMA schemes based on performance and design complexity, polar code construction, encoding and decoding schemes, and different polar decoding algorithms. Further more chapter 2 compares and contrasts existing research on polar coded NOMA schemes and summarizes the technical challenges.

Chapter 3 presents the proposed IDMA-MIMO system model. Chapter 4 presents proposed IDMA-MIMO receiver structure along with mathematical derivations. Chapter 5 presents numerical results obtained through simulation on multiuser MIMO systems and discussion. In chapter 6 directions for future work and concludes the thesis.

Table 1: Notation and Symbols used

Notation/Symbol	Description
$\otimes$	Kronecker product
$()^T$	Transpose operation
$()^H$	Hermitian operation
$\boldsymbol{B}_N$	Permutation matrix
$\boldsymbol{c}^{(m)}$	Polar encoded bit stream of user m
$Cov\Big\{,\Big\}$	Co-variance
$\boldsymbol{d}^{(m)}$	Interleaved chip block of user m
$E\Big\{,\Big\}$	Expected value
$\boldsymbol{G}_N$	Generator matrix
$\Im\Big\{,\Big\}$	Imaginary part of any given complex number
I_o	Number of joint iterations in detection and decoding process
I_d	Number of iterations at BP decoding process
$\Re\Big\{,\Big\}$	Real part of any given complex number
$\mathcal{J}$	Spreaded code block length
K	Information block length
$l_{a,DEC}\left(c^{(m)}\right)$	A priori information produced for polar decoder
$l_{p,DEC}\left(c^{(m)}\right)$	A posterior information produced by polar decoder
$l_{a,MUD}\left(d^{(m)}\right)$	A priori information produced for soft MIMO multiuser detection
$l_{e,MUD}\left(d^{(m)}\right)$	Extrinsic information produced by soft MIMO multiuser detection
$L^m_{s,t}$	Left to right messages of user m
N	Polar coded block length
$P_{Ch,av}$	Average channel gain
$P_{T,av}$	Average transmitted signal power
$\boldsymbol{p}_k^{(m)}$	Chip stream on the k^{th} spatial layer of user m
R_c	Code rate
$R^m_{s,t}$	Right to left messages of user m
$\mathbb{S}$	Spreading factor
$\boldsymbol{s}^{(m)}$	Spreaded chip block of user m
$\boldsymbol{u}^{(m)}$	Bit reversed vector of user m
$Var\Big\{,\Big\}$	Variance
$\boldsymbol{x}^{(m)}$	Symbol vector of user m
π_m	User specific interleaver for user m

Chapter 2

Literature Survey

In this chapter we first summarize the existing research on different NOMA schemes, IDMA and interleaver designing methods. Then summarize polar codes, code construction, encoding and decoding algorithms. We compare successive cancellation decoding and its improved versions with belief propagation decoding. Next, compare and contrast literature on polar coded NOMA schemes.

2.1 Non Orthogonal Multiple Access

This chapter provides a summary of different NOMA schemes. Power domain NOMA and code domain NOMA are two main NOMA categories. Sparse Code Multiple Access (SCMA), Low-Density Spreading CDMA (LDS-CDMA), and Multiuser Shared Access (MUSA) are some code domain NOMA schemes. Pattern Division Multiple Access (PDMA) and Interleave Division Multiple Access (IDMA) are some other types of NOMA schemes. [2, 4].

The power domain NOMA for downlink schemes allocates different power levels for different users. The power allocation depends on their channel conditions [3]. More transmission power will be allocated to the user with a poor channel condition. The Successive Interference Cancellation (SIC) method is employed at the receiver to eliminate multi-user interference. Each user within the cluster needs to decode information from all other users. However high receiver complexity, high energy consumption, and error propagation issues have been identified in the SIC scheme. To achieve the desired performance, the channel gain difference between users should be sufficient, and these issues limit the maximum number of users to be served. Therefore, message passing algorithms (MPAs) have been introduced to reduce the receiver complexity and achieve near-optimal performance by allowing user separation even when the received power levels are comparable [3]. This method is insensitive to the signal to interference noise ratio (SINR) difference of the receiver and also its performance does not degrade with the existence of a user correlation as in SIC receiver [3].

SCMA reduces computational complexity in multiuser detection by achieving the sparsity of the allocation matrix between subcarriers and users [2]. Higher data rates can be achieved with larger sized codebooks, but once the codebook is designed, its data rate becomes fixed, which limits the design of practical SCMA systems. Data rate and reliability are the key concerns of practical SCMA systems [3]. Sparse spreading sequences are employed in LDS-CDMA to reduce the interference at each chip [3]. With the proper spreading sequence design, interference of the multiuser system can be reduced. In MUSA for uplink, each user symbol is spreaded using a spreading sequence [3]. Each user can randomly select a sequence from the pool of multiple spreading sequences. Then using same time frequency resources, all spreading symbols are transmitted. At the receiver, SIC method is employed, to distinguish each user data.

Another type of NOMA scheme is Pattern Division Multiple Access (PDMA) which uses multiple domain non-orthogonal patterns [3, 4]. Therefore, multiplexing can be achieved in either code domain, power domain or in spatial domain, or in any combination of them. Interleave Division Multiple Access (IDMA) uses packet level interleavers to distinguish users [6]. In IDMA different interleavers are used for different users to provide adjacent packets approximately uncorrelated. Summary of different NOMA schemes for uplink is given in Table 2. Interleaver designing methods are discussed in the next section.

Table 2: NOMA schemes

NOMA Scheme	Summary
Power domain NOMA	Allocates different power levels for different users based on their channel conditions, SIC method at receiver
SCMA	Uses the sparsity of the allocation matrix between subcarriers and users, Codeword collisions, Highest computational complexity
LDS-CDMA	Uses sparse spreading sequences to reduce the interference at each chip
MUSA	Uses spreading sequence to spread each user symbols, SIC method at receiver
PDMA	Uses multiple domain non-orthogonal patterns, Pattern collisions, Computational complexity is higher than IDMA
IDMA	Uses different interleavers for different users to provide adjacent packets approximately uncorrelated, No collision. Interleavers are generated independently, Lowest computational complexity

2.1.1 Interleave Division Multiple Access

For IDMA, there are different methods to generate interleavers [8]. This section provides a comparison of different types of interleaver designs including random interleavers, power interleavers, and tree based interleavers are presented. Random interleavers π_k are generated independently for different users. Correlation between interleavers defines the effect of other users' signals on a specific user. The number of interleavers generated at the transmitter increases with the number of users, and similarly, the memory requirement. Therefore, a large storage is required to store those interleavers at both transmitter and receiver. Moreover, large bandwidth is required to exchange interleavers between the transmitter and the receiver in the initial link setup period, which leads to a reduction of spectral efficiency. Therefore, the number of users and the distance between interlevers are the key concerns in system design.

The increase in the bandwidth and memory requirements with the number of users, and the high computational complexity due to user specific interleavers, are the main limitations in IDMA systems. A power interleaver method is proposed as a solution to the extra bandwidth and memory requirement problem, by simplifying the interleaver assignment scheme [8]. It is a serial chip by chip interleaving method that uses a master interleaver (ϕ) and generates a k^{th} inteleaver (π_k) for user k, denoted as (ϕ^k). It only needs to store the master interleaver (ϕ) and intermediate interleaver (π_k) for the ($(k+1)^{th}$) user interleaver calculation. Though this method has reduced the amount of information exchanged between the basestation and the mobile station, it has serial behavior which causes high latency. Therefore, the parallel interleaver design method was proposed in [9] to have low latency with similar performance without memory collision. The proposed parallel interleavers are very similar to random interleavers. This proposed parallel interleaver design method can be used to create the IDMA system and increase system throughput.

A Tree based interleaver (TBI) design method [7] minimizes the computational complexity and memory requirement issues with random and power interleavers. In this method, two master interlaevers are randomly selected. The memory requirement of TBI is much lower as compared to random interleaving whereas it is slightly higher than power interleavers. This method is optimal in terms of bandwidth and bit error rate. The prime interleaver (PI) design approach can be used to further reduce the memory and bandwidth requirements by using a prime number as a seed in the interleaver [8]. As a result, PI has the lowest bandwidth requirement compared to other types of interleavers except TBI. A New Logistic Map (NLM) interleaver was proposed in [10]. It is capable of improving the computational complexity and reducing bandwidth and memory requirements while ensuring secure and infinite sets of codes and interleavers.

2.2 Polar Codes

The concept of polar coding was first proposed by Arikan in 2009 [11]. Mathematical representation of polar code is denoted by (N, K, A) where A is the set of indices of information bits with cardinality K. Polar code construction is the process of selecting these K indices corresponding to high capacity channels out of N channels [11]. Factor graphs with butterfly units are used in polar encoding [11]. This butterfly implementation gives $N(logN)$ complexity. Polar codes are deterministic and have low and fixed complexity, as every codeword has fixed capacity where other capacity approaching codes do not have this fixed complexity and have random bit iterations.

2.2.1 Code Construction

Most commonly used code construction methods are reviewed briefly in this section. Bhattacharyya parameter is the simplest method proposed in [12]. The density evaluation based algorithm uses first-error event probability $P_e(i)$ assuming all zero codewords are transmitted [16]. Puncturing algorithms of [17] generate high rate codes by transmitting only a subset of the code bits, with a rate of K/N mother code. Extending algorithms [17] use the method of retransmission or update the generator matrix with additional columns to generate lower-rate codes from a higher rate mother code.

2.2.2 Polar Code Decoders

There are various polar code decoding algorithms proposed in the literature. In this section, the most common types of decoders are reviewed.

Successive Cancellation (SC) decoding

SC decoder was first proposed in Arikan's paper [11], as the fundamental polar decoder for achieving capacity with moderate complexity. This is a greedy tree search algorithm, selecting one best link every time with capacity achieving performance asymptotically. It is a two-way recursive algorithm. The reliability of the retrieval of source bits is improved by successive cancellation of the interference generated by prior bits. Decoding is done based on the polar code factor graph using log likelihood ratios (LLRs) [11]. Other advanced polar decoding algorithms are developed based on this SC decoding method. Serial nature of SC decoding shows long latency with low throughput. Non-overlapping trees in the factor graph can be decoded simultaneously. Parallelism can be used to reduce computational time and speed up the overall decoding process.

SC-decoder itself could not defeat the maximum likelihood (ML) decoder as its performance is significantly lower than ML decoder. For short to moderate block lengths, polar codes performance is weak. Therefore, polar codes with SC decoding show lesser performance than turbo codes or LDPC codes [18]. Hence, SC-list (SCL) decoding and SC-heap (SCH) decoding algorithms were proposed in [18] to improve the performance of SC decoding, based on path searching and expansion.

Successive Cancellation List (SCL) decoding

The proposed SCL decoding algorithm performs almost same as the ML decoding scheme. It shows the complexity of $O(LNlogN)$ where L denotes the list size, because instead of keeping only one candidate path in each step, it keeps a list of L survival paths. Still polar codes with SCL decoding scheme perform poorer than LDPC codes.

Cyclic redundancy check -aided SCL (CA-SCL)

It has been shown that the polar codes with CA-SCL decoding are capable of achieving better performance than LDPC codes and turbo codes [19]. Its main drawback is high decoding complexity. If there is a certain bit decoded erroneously during the decoding process, the whole process gets erroneous. Therefore, CA-SCL decoder needs an efficient early stopping criteria to reduce the decoding complexity and latency. Segmented CRC-aided SCL (SCA-SCL) decoder is proposed as the solution, with an early stopping scheme as described in [20]. CRC detectors are used at the end of decoding and at other breaking points during the decoding process. With these CRC detectors, the decoder could eliminate invalid paths before reaching the maximum length of the code and remove the unnecessary complexity. The process is considered as a decoding failure if all possible paths were failed to pass the CRC detection and retransmission will be requested.

Successive Cancellation Heap (SCH) decoding

SCH decoding algorithm [18] searches for the best path in the heap, by selecting the path with the maximum metric in the root to expand new paths. After the expansion, insertion of the new paths keeps the maintenance. The time complexity of the insertion is $O(logD)$, where D is the number of nodes in the heap and is only related to the height of the heap. Therefore, SC heap decoding is much better than SC list decoding and the main advantage of SCH over SCL is its ability to store paths with different lengths.

Belief Propagation Decoding

The message passing algorithm (MPA) achieves near optimal performance with tolerable complexity. The BP scheme is a MPA which iteratively updates messages between the user nodes and function nodes. Therefore, soft messages are transferred among user nodes and function nodes in BP decoding rather than exchanging hard messages. In contrast, processing of BP decoding is parallel and processing of SC decoding is serial in nature. Therefore, BP decoding has low latency and is preferred over SC decoding, even though with higher computational complexity compared to SC decoding. Inherited parallelism of the BP decoder provides the possibility of joint processing with other baseband modules: multi user MIMO detector, deinterleaver, and despreader. Therefore, the BP polar decoder has become more favorable for high throughput applications.

2.3 Polar Coded NOMA Schemes

Polar Coded NOMA (PC-NOMA) is one of the promising technologies to meet the requirements of 5G and beyond 5G networks. Improved performance can be obtained by using applications of polar codes with NOMA systems. It uses polar codes with NOMA systems to have better performance with low computational complexity. Nevertheless, in the literature, PC-NOMA has so far received limited attention. This section reviews the PC-NOMA schemes proposed in the literature, paying special attention to the performance and complexity of the NOMA scheme and decoding algorithm used.

A polar coded SCMA system with CRC aided SCL (CA-SCL) polar decoding was proposed in [21]. This is a combination of multilevel coded modulation (MLCM) with multistage decoding. The main idea of this proposed system is to overload subcarriers in a controlled manner. The code rate design of MLCM is based on capacity rules, and the rate of individual coding level is selected in such a way that it equals the equivalent channel capacity. The performance of MLCM with polar codes is better than that of the bit interleaved coded modulation (BICM) with turbo codes, but at the cost of slow convergence leading to a more number of iterations. The computational complexity of MLCM increases with the number of iterations, because the multiuser detection and decoding processes repeat at each stage. Therefore, it is desirable that the iterative process should be terminated at the minimum possible iterations. Number of iterations can be either the number of iterations for a successful CRC or the maximum allowable iterations in the case of no successful CRC before the predefined maximum. Otherwise, processing complexity will be increased unnecessarily.

Conventional polar coded NOMA schemes use separate detection and decoding (SDD) with two separate factor graphs for both detection and decoding [13]. In the first step, detection of the receiving signal is carried out at the multiuser detector to acquire likelihood messages. Then those likelihood messages are transformed from the detector to the decoder for decoding and get the output bit sequence. In contrast, in the joint detection and decoding (JDD) method, likelihood messages pass between the detection and the decoding graphs within the same iteration [13, 14]. This improves decoding because likelihood messages get updated by both graphs iteratively. The JDD scheme proposed in [13] for polar-coded SCMA based NOMA system increases both the convergence speed and error performance even with almost similar complexity and hardware cost of SDD. In [13], belief propagation based MPA, which is capable of achieving near optimal performance with reasonable complexity, was proposed for polar code decoding in SCMA systems. In [13], the hardware complexity of both JDD and SDD schemes were compared. JDD requires an additional memory block to store likelihoods exchanged between the detection and decoding factor graphs. However, this additional implementation cost is negligible compared to the error performance gain. Therefore, the JDD scheme can be used to improve the error performance.

The performance of two NOMA schemes; SCMA and PDMA schemes were discussed based on the transceiver structure, detection method, and decoding algorithm in [12]. In the SCMA transmitter, each user's bit stream is directly mapped into a sparse codeword. SCMA provides massive connectivity by allowing codeword overloading in the codebooks when a number of multiplexed users exceed the orthogonal resources. In the sparse factor graph, users and physical resource elements (PREs) are represented by variable nodes and functional nodes respectively. The degree of freedom (dof) of a virtual node is defined as the number of connected PREs to that virtual node. In SCMA, all the virtual nodes have the same dof, but in PDMA, the dof might be different for each virtual node. This is the main difference between SCMA and PDMA. This irregular degree distribution of PDMA gives an additional polarization effect resulting in better error performance. Thus, use of the necessary optimality conditions is more beneficial for large systems as it reduces search complexity by excluding most invalid orders. The necessary optimality conditions work more efficiently in PDMA than in SCMA [12]. However, additional shaping gain can be achieved in SCMA codebook designing because it is based on joint optimization of sparse spreading codebook and multi-dimensional rotational constellation. But that is impossible with PDMA [7].

A polar coded SCMA system with joint successive cancellation and a polar coded PDMA system with parallel and successive cancellation were proposed in [12]. In the polar coded SCMA scheme, the code rate is different for each user and those with the lower code rate will have higher priority. A joint iterative detection and decoding (JIDD) receiver was proposed for uplink polar coded SCMA system in [22]. The complexity of the JIDD receiver with polar-coded SCMA is much lower than that of turbo coded and LDPC coded SCMA systems. The soft cancellation (SCAN) decoding algorithm is used in the proposed

JIDD receiver [22]. SCAN has the same complexity as BP decoding, but with fast convergence, which leads to low memory requirements. The proposed system uses Bhattacharya parameter bound for polar code construction, the MPA as the SCMA detection algorithm and SCAN as the polar decoding method, with random interleaving. The proposed JIDD scheme for polar coded SCMA system has better performance and less complexity.

The coding block length proposed for the 5G ultra-reliable low latency communications (URLLC) scenario is quite small to meet the low latency constraint. Polar codes perform better than LDPC codes in short lengths. An uplink polar coded SCMA system was proposed in [23] with CRC-SCL decoding and MPA. It concludes that polar coded SCMA outperforms LDPC in short code lengths.

A Turbo coded IDMA system was proposed in [6] . Since polar codes were proposed for enhanced mobile broadband (eMBB) control channels in 5G network (3GPP release 15), recent research has focused on polar coded IDMA systems. It is expected that IDMA can be used to improve the capacity of wireless communication systems. One such polar coded IDMA scheme was proposed in [14]. Polar codes are applied to an OFDM-IDMA system to improve the error performance. Moreover, a Sign-Aided JDD (SA-JDD) scheme was proposed in [14] to further reduce the detection complexity. Detection and decoding iterations can be terminated when signs of LLRs become stable. BP polar decoding is used at the receiver of the proposed polar coded OFDM-IDMA system. As per the results of [14], SA-JDD scheme has better error performance at high SNRs compared to JDD scheme. The early termination method is used in [24] for an IDMA system with SRC-SCL decoding to improve the undetected error rate.

Different polar coded NOMA schemes have been compared and contrasted in this section including NOMA schemes, decoding algorithms, detection and decoding schemes. A summary of discussed polar coded NOMA schemes is given in Table 3.

Table 3: Summary of polar coded NOMA schemes

NOMA scheme	Decoding method	Remark
SCMA	SCD	Advantage - PC-SCMA out performs turbo coded SCMA Disadvantages - All virtual nodes have same degree of freedom, Codeword collision
PDMA	SCD	Necessary optimality conditions work more efficiently in PDMA than in SCMA Advantages - Irregular degree distribution of PDMA gives additional polarization effect and show better performance Necessary optimality conditions reduce search complexity by excluding most invalid orders PC-PDMA out performs turbo coded PDMA Disadvantages - Pattern collision
SCMA	SC-L decoding	Advantages - Performance of multilevel coded modulation (MLCM) with polar codes is better than the performance of bit interleaved coded modulation (BICM) with turbo codes Disadvantages - Slow convergence and computational complexity increases with number of iterations JDD shows almost similar complexity and hardware cost compared to SDD
SCMA	CRC-SCL	The BP algorithm is extended to calculate the extrinsic LLR information Advantages - PC-SCMA outperforms LDPC-SCMA Decoding complexity of polar codes is lower than that of LDPC codes
SCMA	SCAN	Joint Iterative detection and decoding Advantages - Better performance compared to MPA algorithm for SCMA and CA-SCL decoding
SCMA	BP decoding	Joint detection and decoding (JDD) Advantages - Emerging of two factor graphs increases both convergence speed and performance in JDD
IDMA	BP decoding	Sign-aided JDD Advantages - Decoding complexity is reduced due to SA-JDD Performs well in high SNRs
IDMA	CRC-SCL	Early termination Improve UER (Undetected Error Rate)

2.4 Technical Challenges

Recent attention has been driven to IDMA based polar coded NOMA schemes because of IDMA's better performance over other NOMA schemes. However, there is a limited number of research studies on IDMA based polar coded systems and research in this area is still not mature.

BP decoding scheme has low latency due to its parallel nature of processing and therefore it is much preferred for the proposed receiver. However, it has higher complexity than SC decoding.

Separate detection and decoding schemes are used in existing receiver designs. However, recent work tends to use joint detection and decoding schemes to reduce decoding complexity. Merging of detection and decoding factor graphs allows easy flow of likelihood messages and will ultimately improve the error correction capability of the receiver.

Chapter 3

System Model

In this section we describe the polar coded IDMA-MIMO system model for multi-user uplink communication. We consider that there are M users in the system. Each user has M_T number of transmit antennas and M_R number of antennas employed at the basestation receiver.

3.1 Transmitter

The multiuser polar-coded IDMA-MIMO transmitter structure is shown in Fig.1. The transmitter of each user consists of a polar encoder, spreader, interleaver, and serial to parallel converter (S/P).

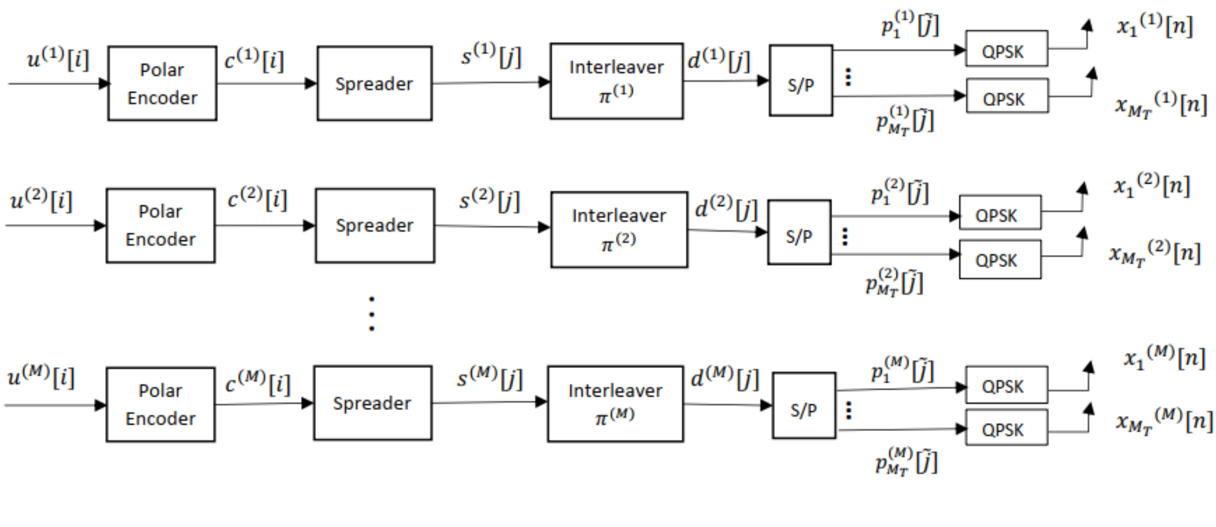

Figure 1: Polar-coded IDMA-MIMO transmitter structure

Let $\boldsymbol{u}^{(m)}$ represent the N long input bit sequence of user m to the polar encoder.

$$\boldsymbol{u}^{(\boldsymbol{m})} = \left(u^{(m)}[o], u^{(m)}[1], \ldots, u^{(m)}[K-1],\, u^{(m)}[N-K], \ldots,\, u[N-1]\right)\ ,\ m = 1, 2, \ldots, M \quad ,$$

where the first K bits $\left\{u^{(m)}[\tilde{i}]\right\}_{\tilde{i}=0}^{K-1}$ represent the information bits and the second $N-K$ bits $\left\{u^{(m)}[\tilde{i}]\right\}_{\tilde{i}=\ N-K}^{N-1}$ represent the frozen bits. Then bit reversal operation is performed on $\boldsymbol{u}^{(m)}$ prior to polar encoding. The polar encoded bit vector of length $N = K/R_c$ is given by

$$\boldsymbol{c}^{(m)} = \boldsymbol{u}^{(m)}\boldsymbol{G}_N \quad , \tag{1}$$

where $\boldsymbol{G}_N$ is the generator matrix and R_c is the code rate. $\boldsymbol{G}_N$ is defined as [11],

$$\boldsymbol{G}_N = \boldsymbol{F}^{\otimes a} \quad ,$$

where $\boldsymbol{F} = \begin{bmatrix} 1 & 0 \\ 1 & 1 \end{bmatrix}$ and $a = log_2 N$.

Spreading is performed on the polar-coded bit vector using a repetition code. The resulting chip block of user m, $\boldsymbol{s}^{(m)}$ is given by,

$$\boldsymbol{s}^{(m)}[j] = \boldsymbol{c}^{(m)}\left[\ \lfloor j/\mathbb{S} \rfloor\ \right] \quad , \tag{2}$$

where $j = 0, 1, \ldots, \mathcal{J} - 1$ and $\mathcal{J} = N \times \mathbb{S}$ and $\mathbb{S}$ is the spreading factor.

The chip block is then interleaved using an user specific random interleaver π_m. The interleaved chip block $\boldsymbol{d}^{(m)}$ is obtained as

$$\begin{aligned} \boldsymbol{d}^{(m)} &= \boldsymbol{s}^{(m)}[\pi_m] \\ &= \left(d^{(m)}[0], d^{(m)}[1], d^{(m)}[2], \ldots, d^{(m)}\left[\mathcal{J} - 1\right]\right). \end{aligned}$$

Next, serial to parallel conversion is performed on $\boldsymbol{d}^{(m)}$ to generate M_T parallel chip streams. Let $\boldsymbol{p}_k^{(m)}[\tilde{j}]$ be the chip stream on the k^{th} spatial layer of user m in the $\tilde{j}^{th}$ chip interval, which is obtained as

$$p_k{}^{(m)}[\tilde{j}] = d^{(m)}\left[\tilde{j}M_T + k - 1\right] \quad , \tag{3}$$

where $\tilde{j} = 0, 1, 2, \ldots, \overline{\mathcal{J}} - 1,\ k = 1, 2, \ldots, M_T$, and $\overline{\mathcal{J}} = \mathcal{J}/M_T$.

The QPSK modulated symbol on the k^{th} spatial layer of user m, $\boldsymbol{x}_k^{(m)}[n]$ is given by,

$$\begin{aligned} \boldsymbol{x}_k^{(m)}[n] &= \left(\tilde{p}_k^{(m)}[2n-1] + i\tilde{p}_k^{(m)}[2n]\right)/\sqrt{2} \\ \boldsymbol{x}_k^{(m)} &= \left(x_k^{(m)}[0], x_k^{(m)}[1], x_k^{(m)}[2], \ldots, x_k^{(m)}\left[\mathcal{Q} - 1\right]\right) \quad , \end{aligned} \tag{4}$$

where $\tilde{p}_k^{(m)}[\tilde{j}] = 2 \times p_k^{(m)}[\tilde{j}] - 1$, $n = 0, 1, 2, \ldots,\ \mathcal{Q} - 1$ and $\mathcal{Q} = \overline{\mathcal{J}}/2$ The QPSK modulated symbol vector $\boldsymbol{x}^{(m)}[n]$ is transmitted by M_T transmit antennas of user m at any given symbol interval n.

$$x^{(m)}[n] = \begin{bmatrix} x_1^{(m)}[n] \\ x_2^{(m)}[n] \\ \vdots \\ x_{M_T}^{(m)}[n] \end{bmatrix} \ , \ m = 1, 2, \ldots, M \tag{5}$$

Similarly, all users transmit their symbol vectors from M_T transmit antennas.

3.2 MIMO Channel Model

We consider a frequency-flat fading spatially uncorrelated MIMO channel for each user in the uplink transmission. The M_R by M_T MIMO channel matrix of user m for a given symbol interval n, $\boldsymbol{H}^{(m)}[n]$ is given by

$$\boldsymbol{H}^{(m)}[n] = \begin{bmatrix} h_{0,0}^{(m)}[n] & h_{0,1}^{(m)}[n] & \ldots & h_{0,M_T-1}^{(m)}[n] \\ h_{1,0}^{(m)}[n] & h_{1,1}^{(m)}[n] & \ldots & h_{1,M_T-1}^{(m)}[n] \\ \vdots & \vdots & \ddots & \\ h_{M_R-1,0}^{(m)}[n] & h_{M_R-1,1}^{(m)}[n] & \ldots & h_{M_R-1,M_T-1}^{(m)}[n] \end{bmatrix}_{M_R \times M_T} ,$$

where $n = 0, 1, 2, \ldots, Q-1$ and $h_{(m_r,m_t)}^{(m)}[n]$ represents the complex valued Rayleigh fading channel coefficients of the sub channel of the (m_r, m_t) transmit-receive antenna pair at the symbol interval n. Each user channel is assumed to be statistically independent. Moreover, each channel coefficient is assumed to be time-invariant within each symbol interval and varies from symbol interval to symbol interval independently.

3.3 Received Signal

We assume that the received signal is sampled at a rate of one sample per symbol interval. The received signal vector $\boldsymbol{r}[n] = (r_1[n], r_2[n], \ldots, r_{M_R}[n])^T$ at symbol interval n, can be given as

$$\boldsymbol{r}[n] = \sum_{m=1}^{M} \boldsymbol{H}^{(m)}[n] \ \boldsymbol{x}^{(m)}[n] + \boldsymbol{w}[n] \ , \tag{6}$$

where $\boldsymbol{w}[n] = (w_1[n], w_2[n], \ldots, w_{M_R}[n])^T$ is the vector of complex AWGN noise samples with zero mean and variance σ_n^2. Noise variance, σ_n^2 can be calculated as follows

$$\sigma_n^2 = \frac{10^{-E_b/N_0} \times \mathbb{S}}{2bR_c} \ , \tag{7}$$

where b represents number of bits per symbol, $b = 2$ for QPSK modulation. The proposed receiver structure with detailed mathematical derivations is presented in the next chapter.

Chapter 4

Proposed Receiver Structure

The proposed polar-coded IDMA-MIMO receiver structure is shown in Fig.2. It consists of a soft-input soft-output (SISO) multiuser MIMO detector and a SISO polar decoder as the main constituent components. The proposed receiver performs soft multiuser MIMO detection and soft polar decoding iteratively by exchanging the extrinsic information of coded bits between the SISO multiuser MIMO detector and the BP polar decoder in the each iteration. The complete algorithm for iterative detection and decoding is given in Algorithm1. Note that the proposed iterative receiver can be considered as an extension to the work of [15]. In [15], soft channel decoders were employed with MIMO multiuser detector.

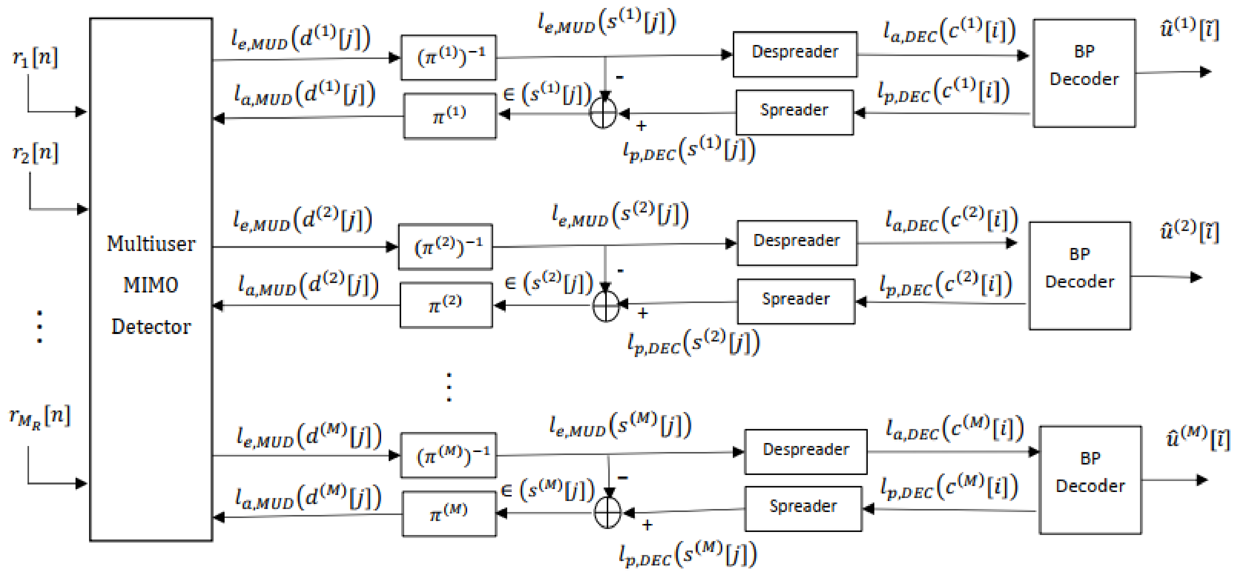

Figure 2: Proposed receiver structure for the polar-coded IDMA-MIMO receiver

We assume that the perfect knowledge of the channel matrix, $\boldsymbol{H}^{(m)}[n]$ is available at the receiver. Let us consider the signal transmitted by the k^{th} antenna of user m as the desired signal, $x_k^{(m)}[n]$. Thus, all the symbols transmitted by the other antennas of user m and all the symbols of the other users transmitted in the n^{th} symbol interval are considered as interference. The received signal vector in (6) can be rewritten as

$$\boldsymbol{r}[n] = \boldsymbol{h}_k^{(m)}[n]\ x_k^{(m)}[n] + \boldsymbol{\eta}_k^{(m)}[n] \quad , \tag{8}$$

where $n = 0, 1, 2, \ldots,\ Q-1$ and $\boldsymbol{h}_k^{(m)}[n]$ denotes the k^{th} column of $\boldsymbol{H}^{(m)}[n]$ and $\boldsymbol{\eta}_k^{(m)}[n]$ denotes the interference plus noise vector at n. We can express $\boldsymbol{\eta}_k^{(m)}[n]$ as follows

$$\boldsymbol{\eta}_k^{(m)}[n] = \sum_{\substack{j_T = 1 \\ j_T \neq k}}^{M_T} \boldsymbol{h}_{j_T}^{(m)}[n] x_{j_T}^{(m)}[n] + \sum_{\substack{v = 1 \\ v \neq m}}^{M} \boldsymbol{H}^{(v)}[n]\boldsymbol{x}^{(v)}[n] + \boldsymbol{w}[n] \tag{9}$$

The first term in (9) denotes the interference due to the symbols transmitted from the other antennas of the same user except the k^{th} antenna. The second term denotes the interference generated due to the symbols transmitted by all the other multiple access users in the system. The received signal $r[n]$ is transformed in to $\tilde{r}[n]$ (10), which is then used in the MIMO multiuser detector to generate the soft output.

$$\tilde{r}[n] \triangleq \left(\boldsymbol{h}_k^{(m)}[n]\right)^H \boldsymbol{r}[n] \tag{10}$$

$$\tilde{r}[n] = \left|\boldsymbol{h}_k^{(m)}[n]\right|^2 x_k^{(m)}[n] + \tilde{\eta}_k^{(m)}[n] \quad , \tag{11}$$

where $n = 0, 1, 2, \ldots,\ Q-1,\ \tilde{\eta}_k^{(m)}[n] = \left(h_k^{(m)}[n]\right)^H \boldsymbol{\eta}_k^{(m)}$.
The signals received from M_R antennas $\boldsymbol{r}[n]$ in (8) are used by the multiuser MIMO detector to make the soft estimates of the chips transmitted by each transmit antenna. The detailed mathematical derivations of the multiuser MIMO detection process are presented in the sequel.
Let $l_{e,MUD}\left(d^{(m)}[j]\right)$ be the extrinsic LLR values of the interleaved chips $\left\{\boldsymbol{d}^{(m)}[j]\right\}_{j=0}^{J-1}$, $m = 1, 2, \ldots, M$, is generated by the multiuser MIMO detector. The deinterleaving operation is performed on $l_{e,MUD}\left(d^{(m)}[j]\right)$ to obtain the LLR value of chip $s^{(m)}[j]$ as

$$l_{e,MUD}\left(s^{(m)}[j]\right) = l_{e,MUD}\left(d^{(m)}(\pi_m^{-1}[j])\right), \quad j = 0, 1, \ldots, J-1. \tag{12}$$

The deinterleaved chip LLR values are used to compute the LLR values of the coded bits

$\left\{c^{(m)}[i]\right\}_{i=0}^{N-1}$ as follows

$$l_{a,DEC}\left(c^{(m)}[i]\right) = \sum_{q=0}^{\mathbb{S}-1} l_{e,MUD}\left(s^{(m)}[i \times \mathbb{S} + q]\right). \tag{13}$$

The despreader output, $\left\{l_{a,DEC}\left(\boldsymbol{c}^{(m)}[i]\right)\right\}_{i=0}^{N-1}$ are used as the a priori LLR values of coded bits for the polar decoder of each user.
Let $\left\{l_{p,DEC}\left(c^{(m)}[i]\right)\right\}_{i=0}^{N-1}$ represent the a posteriori LLR values of the coded bits obtained from the polar decoder after I_d decoding iterations. Spreading is performed on $\left\{l_{p,DEC}\left(c^{(m)}[i]\right)\right\}_{i=0}^{N-1}$ to obtain the LLR values of the chips, $\left\{l_{p,DEC}\left(s^{(m)}[j]\right)\right\}_{j=0}^{J-1}$ as

$$l_{p,DEC}\left(s^{(m)}[j]\right) = \ l_{p,DEC}\left(c^{(m)}\left(\lfloor j/\mathbb{S}\rfloor\right)\right), \quad j = 0, 1, \ldots, J-1. \tag{14}$$

The difference between the extrinsic LLR information $l_{p,DEC}\left(s^{(m)}[j]\right)$ at the spreader output and the extrinsic information $l_{e,MUD}\left(s^{(m)}[j]\right)$ at the despreaded input is given by $\varepsilon\left(s^{(m)}[i]\right)$ as

$$\varepsilon\left(s^{(m)}[j]\right) = l_{p,DEC}\left(s^{(m)}[j]\right) - l_{e,MUD}\left(s^{(m)}[j]\right) \quad , j = 0, 1, \ldots, \ J-1$$

Interleaving is performed on $\left\{\varepsilon\left(s^{(m)}[j]\right)\right\}_{j=0}^{J-1}$ to obtain the a priori LLR values of interleaved chips $\left\{l_{a,MUD}\left(d^{(m)}[\tilde{j}]\right)\right\}_{j=0}^{J-1}$ as follows,

$$l_{a,MUD}\left(d^{(m)}[j]\right) = \varepsilon\left(s^{(m)}\left(\pi_m[j]\right)\right). \tag{15}$$

The a priori LLR values of the chips $\left\{p_k^{(m)}[\tilde{j}]\right\}_{\tilde{j}=0}^{\overline{\mathcal{J}}-1}$ on the k^{th} transmit antenna of user m can be obtained as

$$l_{a,MUD}\left(p_k^{(m)}[\tilde{j}]\right) = l_{a,MUD}\left(d^{(m)}\left[\tilde{j}M_T + k - 1\right]\right), \tag{16}$$

where $\tilde{j} = 0, 1, 2, \ldots, \overline{\mathcal{J}} - 1$, $k = 1, 2, \ldots, M_T$. The next outer iteration begins with the knowledge of $\left\{l_{a,MUD}\left(p_k^{(m)}[\tilde{j}]\right)\right\}_{\tilde{j}=0}^{\overline{\mathcal{J}}-1}$. This process is carried out in each iteration until a specified number of iterations I_o is completed. Note that at the start of the first iteration there is no a priori LLR information $l_{a,MUD}\left(p_k^{(m)}[\tilde{j}]\right)$ available for multiuser MIMO detection. Therefore, $\left\{l_{a,MUD}\left(p_k^{(m)}[\tilde{j}]\right)\right\}_{\tilde{j}=0}^{\overline{\mathcal{J}}-1}$, $k = 0, 1, \ldots, M_T$ are initialized with zero.
The expected value, $E(p_k^{(m)}[\tilde{j}])$ of chip on the k^{th} spatial layer of user m, $p_k^{(m)}[\tilde{j}]$ is calculated as follows.

$$E(p_k^{(m)}[\tilde{j}]) = tanh\left(\frac{l_{a,MUD}\left(p_k^{(m)}[\tilde{j}]\right)}{2}\right) \quad , \tag{17}$$

where $\tilde{j}= 0, 1, 2, \ldots,\ \tilde{\mathcal{J}} - 1$ and $k = 0, 1, \ldots, M_T$. The expected values $E\{\Re\{x_k^{(m)}[n]\}\}$ and $E\{\Im\{x_k^{(m)}[n]\}\}$ of the real part $\Re\{x_k^{(m)}[n]\}$ and imaginary part $\Im\{x_k^{(m)}[n]\}$ of QPSK symbol $x_k^{(m)}[n]$, respectively, can be obtained as follows.

$$\begin{aligned} E\{\Re\{x_k^{(m)}[n]\}\} &= E\{p_k^{(m)}[2n-1]\} \\ E\{\Im\{x_k^{(m)}[n]\}\} &= E\{p_k^{(m)}[2n]\} \quad , \end{aligned}$$

where $n = 0, 1, 2, \ldots,\ Q - 1$. The variance $Var\{\Re\{x_k^{(m)}[n]\}\}$ and $Var\{\Im\{x_k^{(m)}[n]\}\}$ of the real part $\Re\{\boldsymbol{x}_k^{(m)}\}$ and imaginary part $\Im\{x_k^{(m)}[n]\}$ of QPSK symbol $x_k^{(m)}[n]$, respectively, can be obtained as follows.

$$\begin{aligned} Var\{\Re\{x_k^{(m)}[n]\}\} &= 1 - \left[E\{\Re\{x_k^{(m)}[n]\}\}\right]^2 \\ Var\{\Im\{x_k^{(m)}[n]\}\} &= 1 - \left[E\{\Im\{x_k^{(m)}[n]\}\}\right]^2 \quad , \end{aligned} \tag{18}$$

where $n = 0, 1, 2, \ldots, Q - 1$ and $k = 1, 2, \ldots, M_T$. The expected values and covariance values of $x_k^{(m)}[n]$ are used in the multiuser MIMO detector to generate the extrinsic LLR information $l_{e,MUD}\left(d^{(m)[j]}\right)$ $j = 0, 1, \ldots,\ \mathcal{J} - 1$, as shown in the next subsection.

4.1 MIMO Multiuser Detection

In this subsection the multiuser MIMO detection process is described in detail. Multiuser detection is based on the received signal $r[n]$ from M_R receiver antennas and $r[n]$ can be rearranged by separating real and imaginary parts.

$$\begin{aligned} \boldsymbol{r}[n] \ &= \sum_{m=1}^{M} \left(\Re\left\{\boldsymbol{H}^{(m)}[n]\right\}\Re\{\ \boldsymbol{x}^{(m)}[n]\} - \Im\left\{\boldsymbol{H}^{(m)}[n]\right\}\Im\{\ \boldsymbol{x}^{(m)}[n]\}\right) \\ &+ i\sum_{m=1}^{M} \left(\Im\left\{\boldsymbol{H}^{(m)}[n]\right\}\Re\{\ \boldsymbol{x}^{(m)}[n]\ \} + \Re\left\{\boldsymbol{H}^{(m)}[n]\right\}\Im\{\ \boldsymbol{x}^{(m)}[n]\}\right) + \boldsymbol{w}[n] \quad , \end{aligned} \tag{19}$$

where $n = 0, 1, 2, \ldots, Q - 1$. The expected values $E\left(\Re\{\boldsymbol{r}[n]\}\right)$ and $E\left(\Im\{\boldsymbol{r}[n]\}\right)$, of the real part $\Re\{\boldsymbol{r}[n]\}$ and imaginary part $\Im\{\boldsymbol{r}[n]\}$, respectively, can be given as

$$E\{\Re\{\boldsymbol{r}[n]\}\} = \sum_{m=1}^{M} \Re\left\{\boldsymbol{H}^{(m)}[n]\right\}\ E\{\Re\{\ \boldsymbol{x}^{(m)}[n]\}\ \} - \Im\left\{\boldsymbol{H}^{(m)}[n]\right\}\ E\{\Im\{\ \boldsymbol{x}^{(m)}[n]\}\ \} \quad , \textit{ and}$$

$$E\{\Im\{\boldsymbol{r}[n]\}\} = \sum_{m=1}^{M} \Im\left\{\boldsymbol{H}^{(m)}[n]\right\}\ E\{\Re\{\ \boldsymbol{x}^{(m)}[n]\}\ \} + \Re\left\{\boldsymbol{H}^{(m)}[n]\right\}\ E\{\Im\{\ \boldsymbol{x}^{(m)}[n]\}\ \} \quad ,$$

where $n = 0, 1, 2, \ldots, Q-1$. The, covariance matrices $Cov\left(\Re\{\boldsymbol{r}[n]\}\right)$ and $Cov\left(\Im\{\boldsymbol{r}[n]\}\right)$ of the real part $\Re\{\boldsymbol{r}[n]\}$ and imaginary part $\Im\{\boldsymbol{r}[n]\}$, respectively, can be given as

$$
\begin{aligned}
Cov\{\Re\{\boldsymbol{r}[n]\}\} = & \sum_{m=1}^{M}\left(\Re\left\{\boldsymbol{H}^{(m)}[n]\right\}\ Cov\{\Re\{\ \boldsymbol{x}^{(m)}[n]\}\ \}\Re\left\{\boldsymbol{H}^{(m)}[n]\right\}^{T}\right) \\
& + \sum_{m=1}^{M}\left(\Im\left\{\boldsymbol{H}^{(m)}[n]\right\} Cov\{\Im\{\ \boldsymbol{x}^{(m)}[n]\}\ \}\Im\left\{\boldsymbol{H}^{(m)}[n]\right\}^{T}\right) + \sigma_{noise}^{2} \quad , \ and \\
Cov\{\Im\{\boldsymbol{r}[n]\}\} = & \sum_{m=1}^{M}\left(\Im\left\{\boldsymbol{H}^{(m)}[n]\right\} Cov\{\Re\{\ \boldsymbol{x}^{(m)}[n]\}\ \}\Im\left\{\boldsymbol{H}^{(m)}[n]\right\}^{T}\right) \\
& + \sum_{m=1}^{M}\left(\Re\left\{\boldsymbol{H}^{(m)}[n]\right\} Cov\{\Im\{\ \boldsymbol{x}^{(m)}[n]\}\ \}\Re\left\{\boldsymbol{H}^{(m)}[n]\right\}^{T}\right) + \sigma_{noise}^{2} \quad ,
\end{aligned}
$$

where $n = 0, 1, 2, \ldots, Q-1$. The covariance matrix, $\boldsymbol{\psi}[n]$ between $\Re\{\boldsymbol{r}[n]\}$ and $\Im\{\boldsymbol{r}[n]\}$ is calculated as

$$
\begin{aligned}
\boldsymbol{\psi}[n] &= Cov\{\Re\{\boldsymbol{r}[n]\}, \Im\{\boldsymbol{r}[n]\}\} \\
&= \sum_{m=1}^{M}\Re\left\{\boldsymbol{H}^{(m)}[n]\right\}\ Cov\{\Re\{\ \boldsymbol{x}^{(m)}[n]\}\ \}\Im\left\{\boldsymbol{H}^{(m)}[n]\right\}^{T} \\
&- \sum_{m=1}^{M}\Im\left\{\boldsymbol{H}^{(m)}[n]\right\}\left(Cov\{\Im\{\ \boldsymbol{x}^{(m)}[n]\}\ \}\right)\Re\left\{\boldsymbol{H}^{(m)}[n]\right\}^{T} \quad ,
\end{aligned}
\tag{20}
$$

where $n = 0, 1, 2, \ldots, Q-1$. The covariance matrices $Cov\left\{\Re\{\ \boldsymbol{x}^{(m)}[n]\}\right\}$ and $Cov\left\{\Im\{\ \boldsymbol{x}^{(m)}[n]\}\right\}$ of the real part and imaginary part of $\boldsymbol{x}_k^{(m)}[n]$, respectively, can be obtained as follows

$$
\begin{aligned}
Cov\left\{\Re\{\ \boldsymbol{x}^{(m)}[n]\}\right\} &= diag\left(Var\left\{\Re\left\{x_k^{(m)}[n]\right\}\right\}\right) \quad , \ and \\
Cov\left\{\Im\{\ \boldsymbol{x}^{(m)}[n]\}\right\} &= diag\left(Var\left\{\Im\left\{x_k^{(m)}[n]\right\}\right\}\right) \quad ,
\end{aligned}
$$

where $n = 0, 1, 2, \ldots, Q-1$ and $k = 1, 2, .., M_T$. From (11), we can obtain an expression for $\widetilde{\eta}_k^{(m)}[n]$ as

$$
\widetilde{\eta}_k^{(m)}[n] = \boldsymbol{h}_k^{(m)}[n]^{H}\boldsymbol{r}[n] - \left|\boldsymbol{h}_k^{(m)}[n]\right|^{2} x_k^{(m)}[n] \quad , \tag{21}
$$

where $n = 0, 1, 2, \ldots, Q-1$.

The real and imaginary parts of $\widetilde{\eta}_k^{(m)}[n]$, $\Re\left\{\widetilde{\eta}_k^{(m)}[n]\right\}$ and $\Im\left\{\widetilde{\eta}_k^{(m)}[n]\right\}$ can be given as

$$\begin{aligned}\Re\left\{\widetilde{\eta}_k^{(m)}[n]\right\} &= \Re\left\{\boldsymbol{h}_k^{(m)}[n]^H\right\}\Re\{\boldsymbol{r}[n]\} - \Im\left\{\boldsymbol{h}_k^{(m)}[n]^H\right\}\Im\{\boldsymbol{r}[n]\} - \left(\left|\boldsymbol{h}_k^{(m)}[n]\right|^2\right)\Re\left\{x_k^{(m)}[n]\right\}\\ \Im\left\{\widetilde{\eta}_k^{(m)}[n]\right\} &= \Re\left\{\boldsymbol{h}_k^{(m)}[n]^H\right\}\Im\{\boldsymbol{r}[n]\} + \Im\left\{\boldsymbol{h}_k^{(m)}[n]^H\right\}\Re\{\boldsymbol{r}[n]\} - \left(\left|\boldsymbol{h}_k^{(m)}[n]\right|^2\right)\Im\left\{x_k^{(m)}[n]\right\} \quad ,\end{aligned}$$

where $n = 0, 1, 2, \ldots, Q-1$.

The expected values $E\left\{\Re\{\widetilde{\eta}_k^{(m)}[n]\}\right\}$ and $E\left\{\Im\{\widetilde{\eta}_k^{(m)}[n]\}\right\}$ of the real part $\Re\left\{\widetilde{\eta}_k^{(m)}[n]\right\}$ and imaginary part $\Im\left\{\widetilde{\eta}_k^{(m)}[n]\right\}$ of $\widetilde{\eta}_k^{(m)}[n]$, respectively, can be obtained as

$$\begin{aligned}E\{\Re\{\widetilde{\eta}_k^{(m)}[n]\}\} &= \Re\left\{\boldsymbol{h}_k^{(m)}[n]^H\right\}E\{\Re\{\boldsymbol{r}[n]\}\} - \Im\left\{\boldsymbol{h}_k^{(m)}[n]^H\right\}E\{\Im\{\boldsymbol{r}[n]\}\}\\ &\quad - \left|\boldsymbol{h}_k^{(m)}[n]\right|^2 E\{\Re\left\{x_k^{(m)}[n]\right\}\}\\ E\{\Im\{\widetilde{\eta}_k^{(m)}[n]\}\} &= \Re\left\{\boldsymbol{h}_k^{(m)}[n]^H\right\}E\{\Im\{\boldsymbol{r}[n]\}\} + \Im\left\{\boldsymbol{h}_k^{(m)}[n]^H\right\}E\{\Re\{\boldsymbol{r}[n]\}\}\\ &\quad - \left|\boldsymbol{h}_k^{(m)}[n]\right|^2 E\{\Im\left\{x_k^{(m)}[n]\right\}\} \quad ,\end{aligned}$$

The variance $Var\left\{\Re\{\widetilde{\eta}_k^{(m)}[n]\}\right\}$ and $Var\left\{\Im\{\widetilde{\eta}_k^{(m)}[n]\}\right\}$ of $\Re\left\{\widetilde{\eta}_k^{(m)}[n]\right\}$ and $\Im\left\{\widetilde{\eta}_k^{(m)}[n]\right\}$ of $\widetilde{\eta}_k^{(m)}[n]$, respectively, can be obtained as

$$\begin{aligned}Var\{\Re\{\widetilde{\eta}_k^{(m)}[n]\}\} &= \Re\left\{\boldsymbol{h}_k^{(m)}[n]^H\right\}Cov\{\Re\{\boldsymbol{r}[n]\}\}\,\Re\left\{\boldsymbol{h}_k^{(m)}[n]\right\}\\ &\quad - \Im\left\{\boldsymbol{h}_k^{(m)}[n]^H\right\}Cov\{\Im\{\boldsymbol{r}[n]\}\}\,\Im\left\{\boldsymbol{h}_k^{(m)}[n]\right\}\\ &\quad + 2\left(\Re\left\{\boldsymbol{h}_k^{(m)}[n]^H\right\}\,\boldsymbol{\psi}[n]\,\Im\left\{\boldsymbol{h}_k^{(m)}[n]\right\}\right) - \left(\left|\boldsymbol{h}_k^{(m)}[n]\right|^2\right)^2 Var\{\Re\left\{x_k^{(m)}[n]\right\}\}\\ Var\{\Im\{\widetilde{\eta}_k^{(m)}[n]\}\} &= \Re\left\{\boldsymbol{h}_k^{(m)}[n]^H\right\}Cov\{\Im\{\boldsymbol{r}[n]\}\}\,\Re\left\{\boldsymbol{h}_k^{(m)}[n]\right\} -\\ &\quad \Im\left\{\boldsymbol{h}_k^{(m)H}\right\}Cov\{\Re\{\boldsymbol{r}[n]\}\}\,\Im\left\{\boldsymbol{h}_k^{(m)}[n]\right\}\\ &\quad - 2\left(\Re\left\{\boldsymbol{h}_k^{(m)}[n]^H\right\}\,\boldsymbol{\psi}[n]\,\Im\left\{\boldsymbol{h}_k^{(m)}[n]\right\}\right) - \left(\left|\boldsymbol{h}_k^{(m)}[n]\right|^2\right)^2 Var\{\Im\left\{x_k^{(m)}[n]\right\}\} \quad ,\end{aligned}$$

We can show that the conditional probability density function of $\tilde{r}[n]$ given $x_k^{(m)}[n]$, $p\left(\tilde{r}[n]|x_k^{(m)}[n]\right)$ is normally distributed with mean $\left(\left|\boldsymbol{h}_k^{(m)}[n]\right|^2 x_k^{(m)}[n] + E\left\{\widetilde{\eta}_k^{(m)}[n]\right\}\right)$ and variance $Var\left\{\widetilde{\eta}_k^{(m)}[n]\right\}$. LLR values, $l_{e,MUD}\left(p_k^{(m)}[2n-1]\right)$ and $l_{e,MUD}\left(p_k^{(m)}[2n]\right)$ can be calculated as follows

$$\begin{aligned}l_{e,MUD}\left(p_k^{(m)}[2n]\right) &= 2\left(\left|\boldsymbol{h}_k^{(m)}[n]\right|^2\right)Var\left\{\Re\{\widetilde{\eta}_k^{(m)}[n]\}\right\}^{-1}\left(\Re\{\tilde{r}[n]\} - E\left\{\Re\{\widetilde{\eta}_k^{(m)}[n]\}\right\}\right)\\ l_{e,MUD}\left(p_k^{(m)}[2n+1]\right) &= 2\left(\left|\boldsymbol{h}_k^{(m)}[n]\right|^2\right)Var\left\{\Im\{\widetilde{\eta}_k^{(m)}[n]\}\right\}^{-1}\left(\Im\{\tilde{r}[n]\} - E\left\{\Im\{\widetilde{\eta}_k^{(m)}[n]\}\right\}\right) \quad ,\end{aligned} \tag{22}$$

where $n = 0, 1, 2, \ldots, Q-1$. The extrinsic LLR information of $d^{(m)}[j]$, generated by the multiuser MIMO detector $l_{e,MUD}\left(d^{(m)}[j]\right)$ can be obtained from $l_{e,MUD}\left(p_k^{(m)}[\tilde{j}]\right)$ in (22) as

$$l_{e,MUD}\left(d^{(m)}[j]\right) = l_{e,MUD}\left(p_k^{(m)}[\lfloor j/M_T \rfloor]\right) \quad , \tag{23}$$

where $j = 0, 1, 2, \ldots, \mathcal{J}-1$, $\mathcal{J} = N \times \mathbb{S}$, and $k = (j \bmod M_T)+1$. The set of M polar decoders operated independently and hence, can operate parallelly in practical implementation.

4.2 BP polar decoding

There is a separate BP algorithm-based polar decoder for each individual user. Note that the set of M polar decoders operate independently and hence, can run in parallel in practical implementation. There are $(b+1)$ number of stages in the factor graph used for BP polar decoding, where $b = \log_2 N$. Factor graph node can be represented by (s, i), where $s = 1, 2, \ldots, b+1$ denotes the stage number and $i = 0, 1, \ldots, N-1$ denotes the node number. There are two types of LLRs defined at any given node (s, i): right to left message $R_{s,i}^{(m)}$ and left to right message $L_{s,i}^{(m)}$ of user m [14]. First, $L_{b+1,i}^{(m)}$ and $R_{1,i}^{(m)}$ are initialized as

$$\begin{aligned} L_{n+1,i}^{(m)} &= l_{a,DEC}\left(c^{(m)}[i]\right) \quad , \\ R_{1,i}^{(m)} &= \left\{ \begin{array}{ccc} 0 \ , & if & i \in A \\ +\infty \ , & if & i \in A^c \end{array} \right\} \end{aligned} \tag{24}$$

where $i = 0, 1, \ldots, \ N-1$, A is the set of indices of the information bits with cardinality K, and A^c is the set of indices of the frozen bits with cardinality $N-K$. Then, the iterative decoding process begins. In each iteration, first all the L messages are updated from the last stage to the first stage and next all the R messages are updated from the first stage to the last stage [13]. The a posteriori LLR of coded bit $c^{(m)}[i]$ obtained after I_d iterations, can be calculated as

$$l_{p,DEC}\left(c^{(m)}[i]\right) = L_{b+1,i}^{(m)} + R_{b+1,i}^{(m)} \quad , \tag{25}$$

where $t = 0, 1, \ldots, \ N-1$. Note that the LLR values $\{l_{p,DEC}\left(c^{(m)}[i]\right)\}_{i=0}^{N-1}$ is used to obtain the a priori information for the multiuser MIMO detection after performing spreading (14) and interleaving (15) operations as previously explained. The LLR values are expected to converge after a few outer iterations (I_o). The hard estimates of the information bits

$\{u^{(m)}[i]\}_{i=0}^{K-1}$ are made based on the following criteria

$$\hat{u}^{(m)}[i] = \begin{cases} 1, & if \quad L_{1,i}^{(m)} \leq 0 \\ 0, & if \quad L_{1,i}^{(m)} > 0 \end{cases} \quad , \tag{26}$$

where $i = 0, 1, \ldots,\ K-1$. The information bits can be filtered out easily by using the set of information bit indices, A which is known to the receiver. The complete algorithm is shown in Algorithm 1. The g function used in BP decoding algorithm can be expressed as follows.

$$g(x, y) \ = sign(x) \times sign(y) \times min(\,|x|\,,|y|\,) \tag{27}$$

Algorithm 1: Joint detection and decoding algorithm

Initialize: $\left\{ l_{a,MUD}\left(\boldsymbol{d}^{(m)}\right)\right\}_{m=1}^{M} = 0$
for i_o=1:I_o **do**
    Calculate $\left\{ l_{e,MUD}\left(\boldsymbol{d}^{(m)}\right)\right\}_{m=1}^{M}$ using eq. (23)
    for m=1:M **do**
        Perform de-interleaving using eq. (12)
        Perform despreading using eq. (13)
        Feed $l_{a,DEC}\left(\boldsymbol{c}^{(m)}\right)$ in iterative BP decoding
        Initialize: $R_{1,i}^{(m)}$ and $L_{b+1,i}^{(m)}$ (24)
        for i_d=1:I_d **do**
            Update L messages
            for s=b:-1:1 **do**
                for i=1:N **do**
                    $L_{s,i}^{(m)} = g\Big(L_{s+1,i}^{(m)}, \Big(L_{s+1,i+N/2}^{(m)} + R_{s,i+N/2}^{(m)}\Big)\Big)$
                    $L_{s,i+N/2}^{(m)} = g\Big(R_{s,i}^{(m)}, L_{s+1,i}^{(m)}\Big) + L_{s+1,i+N/2}^{(m)}$
                end for
            end for
            Update R messages
            for s=1:b **do**
                for i=1:N **do**
                    $R_{s+1,i}^{(m)} = g\left(R_{s,i}^{(m)}, \left(L_{s+1,i+N/2}^{(m)} + R_{s,i+N/2}^{(m)}\right)\right)$
                    $R_{s+1,i+N/2}^{(m)} = g\Big(R_{s,i}^{(m)}, L_{s+1,i}^{(m)}\Big) + R_{s,i+N/2}^{(m)}$
                end for
            end for
        end for
        $l_{p,DEC}\left(\boldsymbol{c}^{(m)}[i]\right) = L_{b+1,i}^{(m)} + R_{b+1,i}^{(m)}$
        Perform interleaving and spreading using eqs.(14)-(15)
    end for
    Use $\left\{ l_{a,MUD}\left(d^{(m)}\right)\right\}_{m=1}^{M}$ for next iteration
end for

Chapter 5

Simulation Results and Discussion

This chapter presents simulation results and discussion. We investigate the error performance of the proposed polar coded IDMA-MIMO system for flat fading channels. We assume that the multiuser uplink MIMO channel matrix is time invariant within each symbol interval and varies from symbol to symbol. The common system parameters considered for simulation are summarized in Table 4. As explained in the chapter 3, the proposed iterative receiver consists of an iterative soft detector and a belief propagation decoder. Bit error rate (BER) performance of IDMA-MIMO systems for various scenarios have been analyzed based on E_b/N_0 values.

Table 4: Common system parameters used for simulations

Parameter	Value
Information block length	$K = 512$
Code rate	$R_c = 0.5$
Spreading factor	$\mathbb{S} = 16$
Interleaving scheme	random
Number of joint iterations in detection and decoding process	$I_o = 5$
Number of iterations at BP decoding process	$I_d = 10$

In Fig. 3, we compare the BER performance of polar codes and LDPC codes for a single user single input single output (SISO) system over AWGN channels. An LDPC code with information block length K =512 and code length N =1024 is considered. BP decoding with 20 iterations is adopted for LDPC codes. It can be observed that polar codes offers considerably improved error performance over LDPC codes for the considered code length and BP decoding.

In Fig.4, we study the BER performance of polar coded 2×2 MIMO systems for single user, 2 users and 4 users scenarios. For comparison purpose, we also include the BER performance of uncoded 2×2 MIMO systems, keeping all the other parameters unchanged

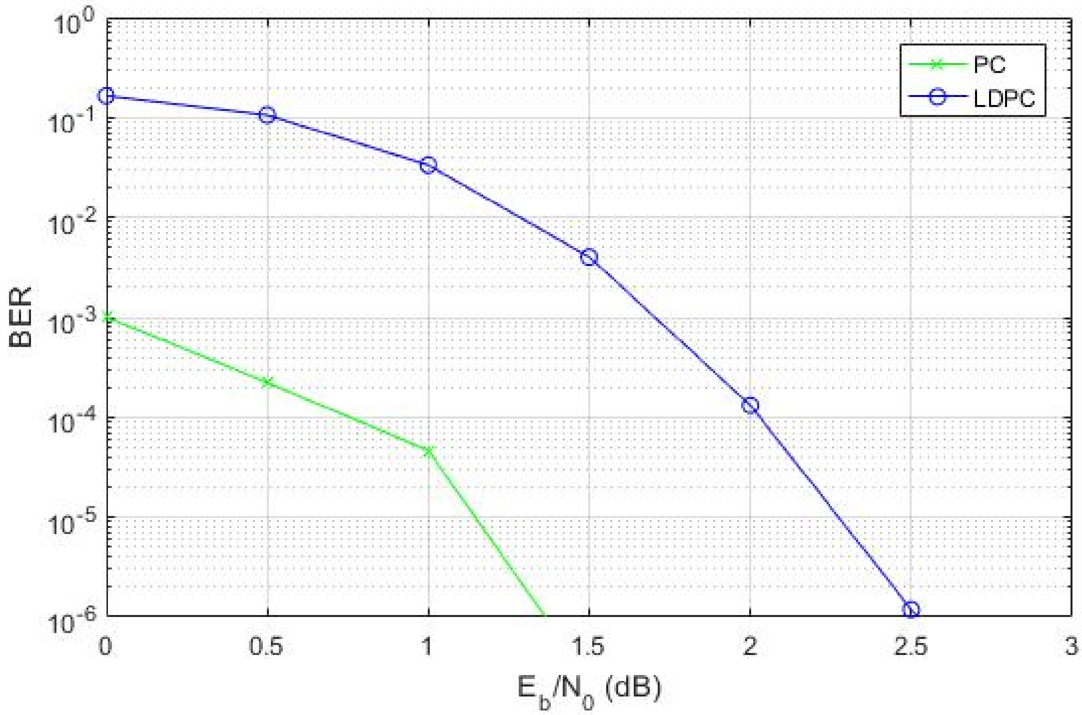

Figure 3: BER performance comparison of polar codes and LDPC codes for single user SISO systems

as in the coded system. The BER is averaged over all users in the system for multiple user scenarios. As expected, considerably improved BER performance can be observed using polar codes in IDMA MIMO systems for high E_b/N_0, about 5 dB. Further we can observe that at a BER of 10^{-3}, a performance improvement of about 4 dB is achieved using polar codes compared to the uncoded system. Moreover, for comparison purposes, we show the performance of a polar-coded 2×2 MIMO system obtained using a single-pass (non-iterative) receiver with single user, two users, and four users. It can be observed that a considerable performance improvement can be obtained using the proposed iterative receiver compared to the single-pass receiver. The performance gain obtained using the proposed receiver compared to the non-iterative receiver increases with the number of users.

In Fig. 5 and Fig.6, we analyze the BER performance of polar coded 2×2 MIMO system and polar coded 4×4 MIMO system respectively for different number of multiple access users in the system. In Fig.5, a single user 2×2 MIMO system is shown as the reference performance. It can be seen that the BER of about 10^{-4} is achieved for 16 users in a 2×2 MIMO system at 9 dB whereas a single user 2×2 MIMO system achieves the same BER performance at about 7 dB. It can be seen that the performance degradation due to multiuser interference is insignificant until 4 users. At a BER of 10^{-3}, compared to the single-user system, the performance degradation is about 0.75 dB and 1.25 dB for 8 and 12

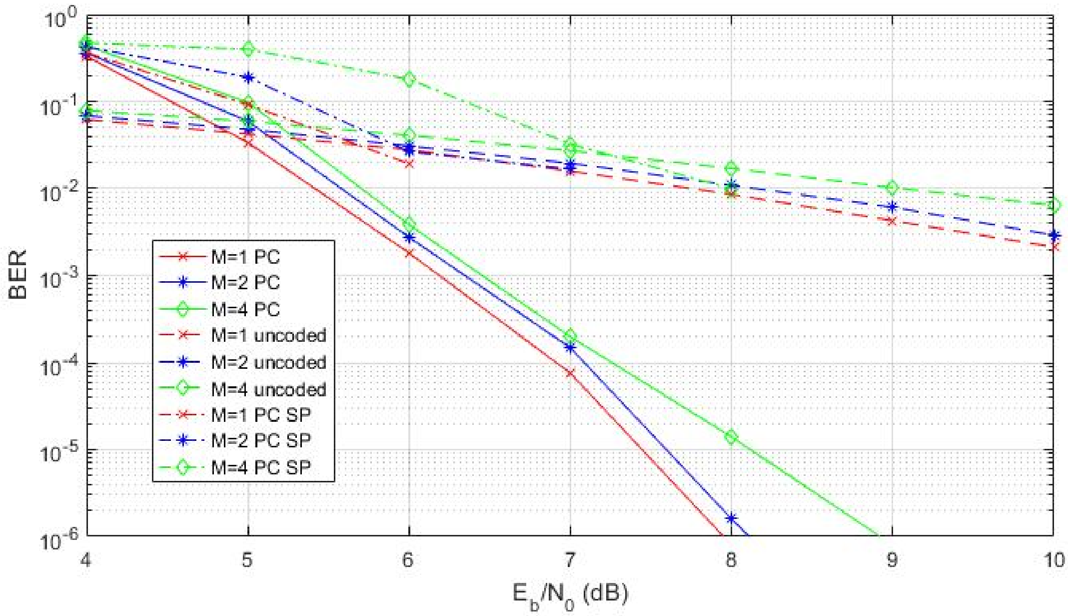

Figure 4: BER performance comparison of polar coded and uncoded 2×2 MIMO systems

users systems respectively.

In Fig. 6 the BER performance obtained for a single user 4 × 4 MIMO system is shown for comparison purpose. We can observe that the BER of about 10^{-4} is achieved by 8 users 4 × 4 MIMO system at 12 dB, whereas the single user system achieves the same BER performance at about 10 dB. In both scenarios, 8 users MIMO system achieves a BER of about 10^{-4} for an additional 2 dB increase compared to single user MIMO systems. It can be seen that the performance degradation due to multiuser interference is insignificant until 4 users. At a BER of 10^{-3}, compared to the single-user system, the performance degradation is about 0.75 dB and 1.5 dB for 8 and 12 users systems respectively.

In Fig. 7 we investigate the BER performance of 4 users polar coded systems with different antenna configurations with different MIMO configurations: 2×2 MIMO, 4×4 MIMO, and 8×8 MIMO systems. We include the BER performance obtained for polar coded single input single output (SISO) system with 4 users as the reference performance. When considering the BER range of 10^{-1} to 10^{-4}, we can observe almost 1.5 times increase of E_b/N_0 value for a given BER, with the increase of M_t and M_r since the spatial interference increases. As expected, the BER performance reduces with the number of transmit antennas increasingly within a BER range of 10^{-1} to 10^{-4}, it can be observed that when the number of antennas is doubled, the performance is degraded by about 1.5 dB. For comparison purposes, the performance obtained using a single-pass (non-iterative) receiver is also shown for different antenna configurations. A considerable BER performance improvement can be observed using the proposed iterative receiver compared to the single-pass receiver for the

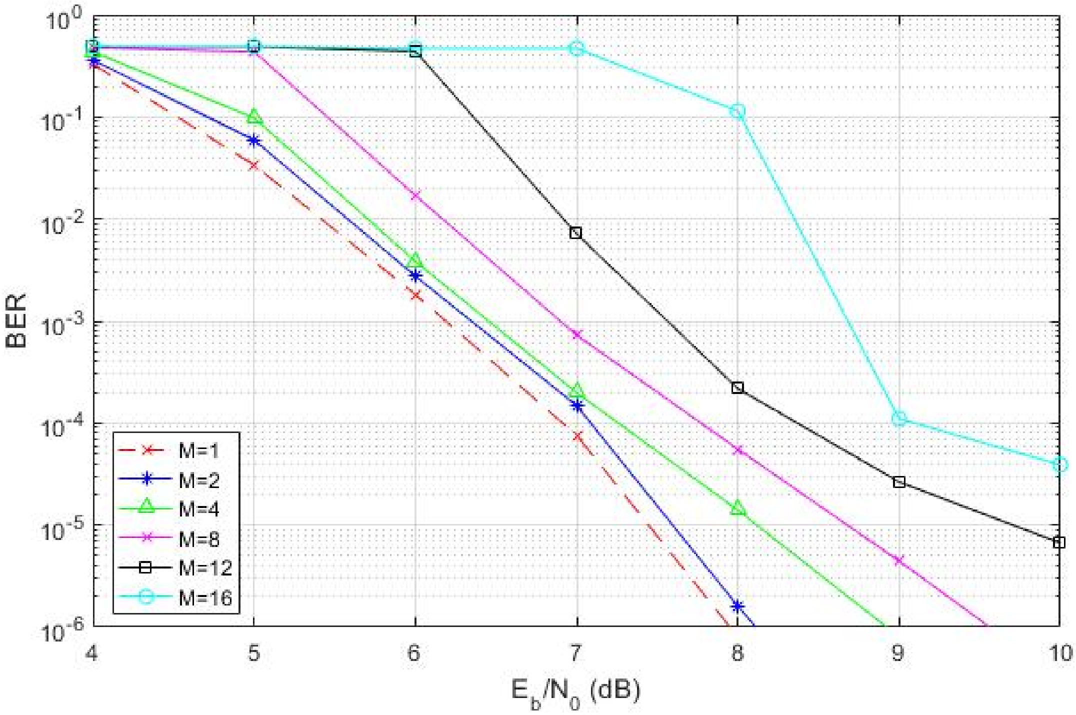

Figure 5: BER performance of polar coded 2×2 MIMO systems with different number of users.

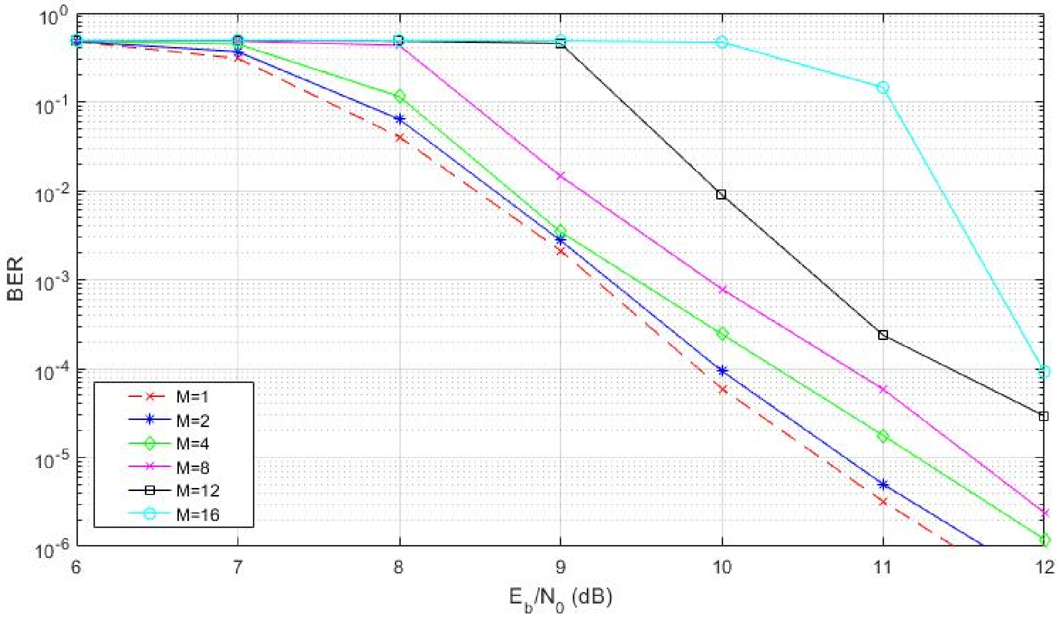

Figure 6: BER performance of polar coded 4×4 MIMO systems with different number of users.

different antenna configurations considered. For a 4×4 MIMO system, at a BER of 10^{-3}, the performance gain of about 2 dB obtained using the proposed iterative receiver compared to the single-pass receiver. Moreover, we can observe a drastically reduced error floor obtained using the proposed iterative receiver compared to the single-pass receiver.

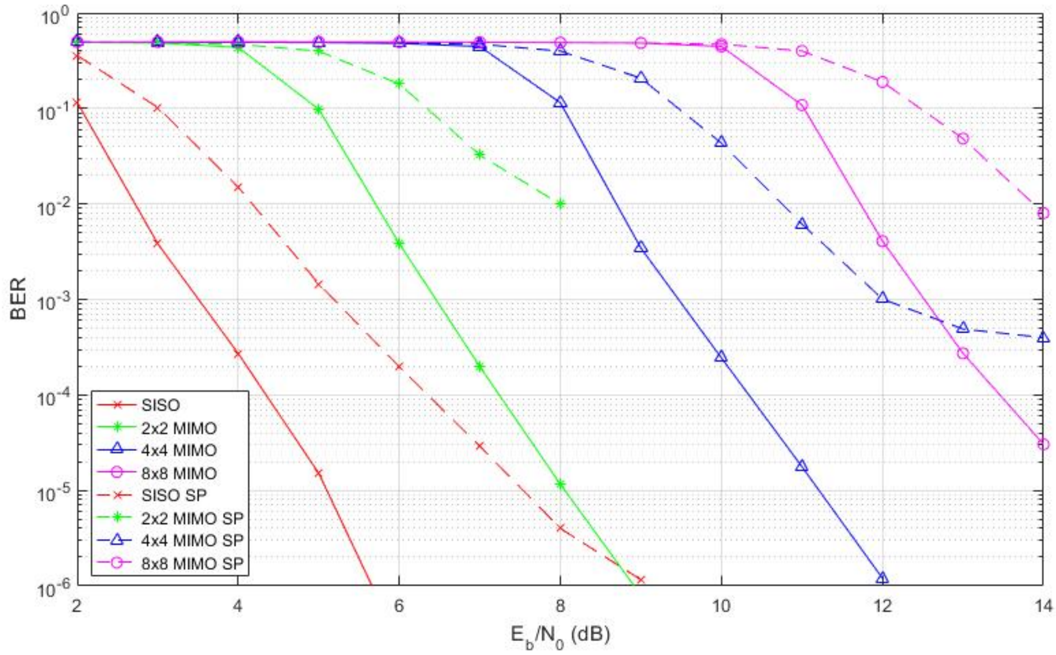

Figure 7: BER performance of 4 users polar coded systems with different antenna configurations

The impact of the number of used iterations in the iterative detection and decoding receiver on the BER performance is studied in Fig. 8. We consider a polar coded 4×4 MIMO system with four users. Here we show the BER performance after each iteration up to a maximum of 5 iterations, ($Ir = 5$). We can observe that up to E_b/N_0 of 6 dB there is no noticeable improvement in the BER with the number of iterations. However, starting from E_b/N_0 of 8 dB the BER reduces with the number of iterations. For E_b/N_0 of 9 dB and above, significant reduction of the BER can be observed in the second iteration from the first iteration. Moreover, from Fig.8, we can see that there is no noticeable improvement in the BER performance after three iterations for high E_b/N_0 values. It can be observed that the higher the E_b/N_0 value, the faster the convergence is.

In Fig.9, we investigate the effect of spreading factor (SF) on the BER performance of a polar coded 4×4 MIMO system with 4 users and 8 users. We can see that higher the spreading factor the better BER performance for a given E_b/N_0 value is. This is due to that the overall coding rate $R_{OA} = R_c/SF$ decreases with the SF. The R_{OA} is 1/16, 1/32 1/64, and 1/128 for $SF = 4, 8, 16, 32,$ and 64, respectively. We can observe that with

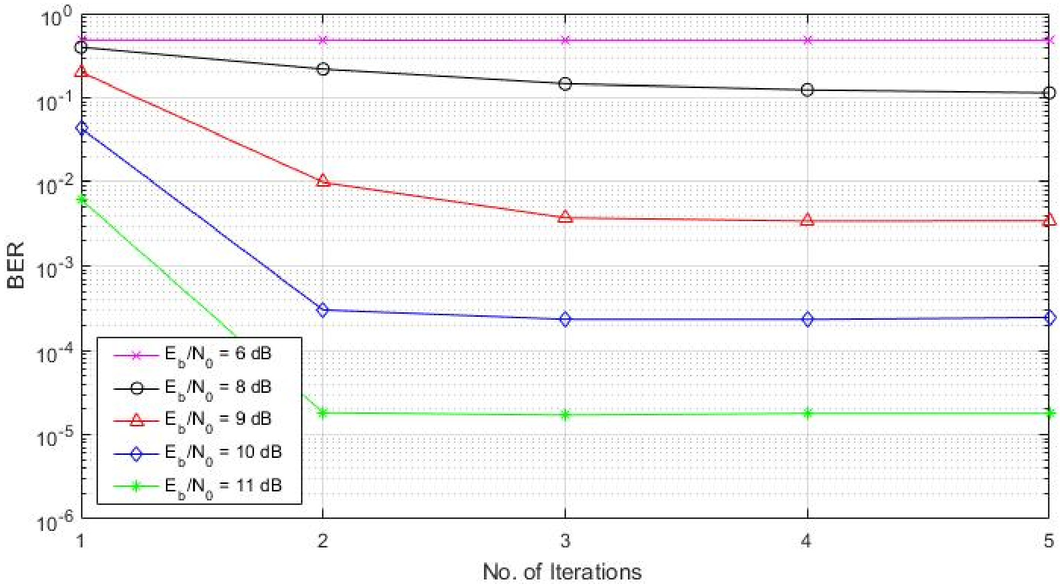

Figure 8: Variation of the BER performance with the number of detection-decoding iterations, in a polar coded 4×4 MIMO system with 4 users

$M = 4$ users when the SF is reduced from 32 to 16, at BER of 10^{-3} the performance degradation is not significant. With $M = 8$ users, when the SF is reduced from 32 to 16, at BER of 10^{-3} the performance degradation is around 0.5 dB. Moreover, with $M = 4$ users the performance improvement obtained by increasing the SF from 8 to 16 is around 0.3 dB. For $M = 8$ users with the $SF = 16$, about 0.5 dB higher E_b/N_0 is required to achieve 10^{-3} compared to $M = 4$ users. For a system with a fixed chip rate (i.e., a fixed sampling rate), the spectral efficiency decreases with the SF since the overall code rate decreases with the SF. Moreover, the computational complexity per symbol increases with the SF since the number of chips per symbol which need to be processed increases with the SF. Thus, even though improved error performance can be obtained with a high SF, a moderate value of SF giving a better tradeoff between the performance and computational complexity/spectral efficiency is preferred.

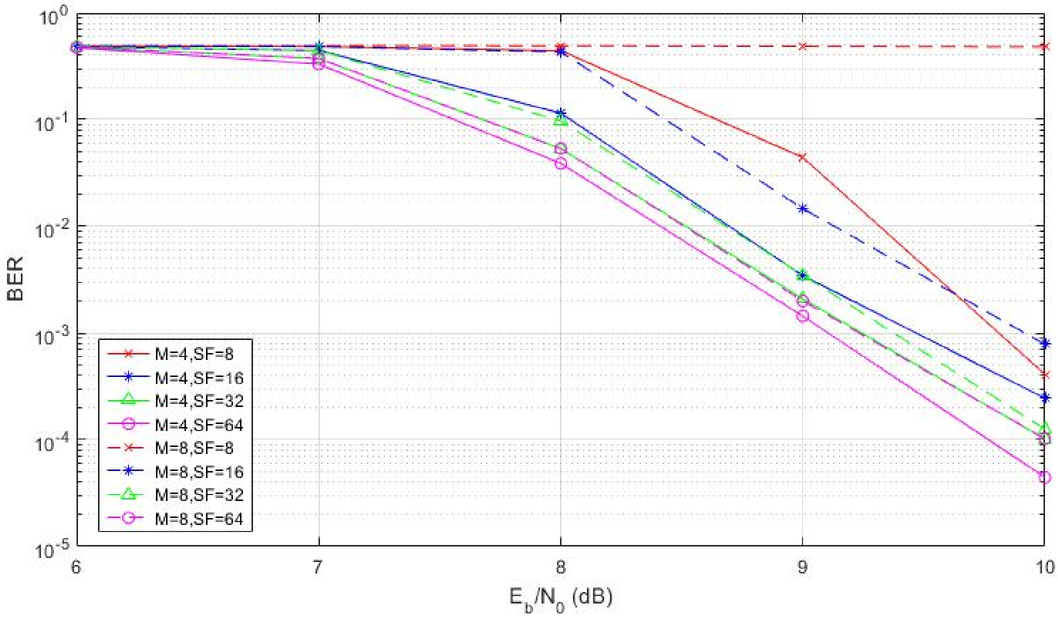

Figure 9: Variation of the BER performance with the spreading factor, in a polar coded 4×4 MIMO systems

Chapter 6

Conclusion and Further Work

6.1 Conclusion

In this thesis a polar coded IDMA-MIMO system has been proposed for multiuser uplink communication. The proposed transmitter consists of a polar encoder, spreader, interleaver, serial to parallel converter, and a set of parallel QPSK modulators. The proposed receiver consists of a soft multiuser MIMO detector, interleaver, de-interleaver, spreader, despreader, and BP polar decoder. An iterative receiver, which consists of a soft multiuser MIMO detector and a BP polar decoder, has been developed. The work of this thesis can be considered as an extension to the work of [15]. In [15], an IDMA-MIMO system was considered with convolutional coding and BPSK modulation, whereas in this thesis polar coding has been considered with QPSK modulation. In [15] receiver, a soft multiuser detector and soft channel decoder were considered whereas in this thesis a soft multiuser MIMO detector and BP polar decoder have been considered respectively. In the proposed iterative receiver, soft messages can be exchanged between modules within the same iteration. This allows iterative detection and decoding.

The key assumptions made in this research study can be summarized as follows:

- The MIMO uplink channel of each user was subject to frequency flat fading and spatially uncorrelated.
- Multiuser uplink MIMO channel matrix is assumed to be time invariant within each symbol interval and varies from symbol to symbol independently (i.e., time uncorrelated).
- Single carrier system is considered for the system model.

The BER performance of the proposed polar coded IDMA-MIMO system have been studied using simulation for various scenarios with different system parameters. The key observations made can be summarized as follows.

- The BER performance of the polar coded systems varies with E_b/N_0. The higher the E_b/N_0 value, the better the BER performance is. The proposed polar coded IDMA-MIMO system has significantly improved BER performance compared to an uncoded IDMA-MIMO system, especially at moderate to high E_b/N_0 values. It can be observed that at a BER of 10^{-3}, a performance improvement of about 4 dB is achieved using polar codes compared to the uncoded system.

- For a given MIMO configuration, the BER increases with the number of multiple access users in the IDMA-MIMO system since the multiuser interference increases. However, the simulation results show that the BER of about 10^{-4} for 16 users 4×4 MIMO system at 12 dB, whereas the single user system achieves the same BER performance at about 10 dB.

- For a given number of multiple access users, the BER increases with the number of transmit antennas. However, the simulation results have clearly demonstrated that the BER of about 10^{-4} for 4×4 MIMO system with 16 users at 12 dB.

- The BER performance increases with the number of detection and decoding iterations at the receiver. The results demonstrated that the higher the E_b/N_0 value, the faster the convergence rate is. The proposed iterative receiver achieves the convergence fast. For example, at moderate E_b/N_0 values significant reduction of the BER can be observed in the second iteration from the first iteration.

- The BER performance increases with the spreading factor as noise variance increases with spreading factor.

The proposed iterative receiver can be used to obtain considerably improved error performance over the single-pass non-iterative receiver. Even though NOMA has not been adopted in the finalized releases of 5G NR specifications, IDMA will be a potential multiple access candidate for beyond 5G mobile communication networks.

As per the research studies, low latency can be achieved by employing BP decoder at the receiver because of its parallel nature of processing compared to SCD. Further in IDMA, interleaver designing has comparatively low computation complexity.

6.2 Further Work

The important directions for further research as extensions to the research work presented in this thesis are identified as follows:

- Flat fading channels are considered in the system model. As for the further work, the polar coded IDMA-MIMO multiuser system analysis can be extended to frequency selective channels.

- QPSK modulation is used in the proposed system. An extension to general MPSK modulation can be considered as an important direction for further work.

- In the proposed IDMA-MIMO system model, single carrier transmission is considered. Another important direction for further research is an extension to OFDMA-based multicarrier transmission.

- The performance of the proposed polar coded IDMA-MIMO system with the iterative receiver scheme was investigated using simulation. A mathematical framework can be developed to analyze the performance theoretically as a component of further work.

Bibliography

[1] 3GPP, "Technical specification of nr for multiplexing and channel coding [ts 38.212]," vol. V15.1.1, 04 2018.

[2] C. Zhang, Y. Huang, F. Sheikh, and Z. Wang, "Advanced Baseband Processing Algorithms, Circuits, and Implementations for 5G Communication," *IEEE Journal on Emerging and Selected Topics Circuits and Systems*, vol. 7, no. 4, pp. 477–490, December 2017.

[3] L. Dai, B. Wang, Y. Yuan, S. Han, C. I, and Z. Wang, "Non–orthogonal multiple access for 5G: solutions, challenges, opportunities, and future research trends," *IEEE Communications Magazine*, vol. 53, no. 9, pp. 74–81, September 2015.

[4] Z. D. et al., "Application of non–orthogonal multiple access in lte and 5G networks," *IEEE Communications Magazine*, vol. 55, no. 2, pp. 185–191, February 2017.

[5] J. Yang, C. Zhang, H. Zhou, and X. You, "Pipelined belief propagation polar decoders," *2016 IEEE International Symposium on Circuits and Systems (ISCAS)*, pp. 413–416, 2016.

[6] L. Ping, L. Liu, K. Wu, and W. K. Leung, "Interleave division multiple–access," *IEEE Transactions on Wireless Communications*, vol. 5, no. 4, pp. 938–947, April 2006.

[7] Z. Wu, K. Lu, C. Jiang, and X. Shao, "Comprehensive study and comparison on 5G NOMA schemes," January 2018.

[8] K. Choudhary and P. Sharma, "Interleavers for IDMA technology: A comparison survey," vol. 1, April 2012.

[9] S. Wu, X. Chen, and S. Zhou, "A parallel interleaver design for IDMA systems," *2009 International Conference on Wireless Communications Signal Processing*, pp. 1–5.

[10] B. Akbil and D. Aboutajdine, "Improved IDMA for multiple access of 5G," *International Journal of Communication Networks and Information Security*, vol. 7, no. 3, 2015.

[11] E. Arikan, “Channel Polarization: A Method for Constructing Capacity–Achieving Codes for Symmetric Binary–Input Memoryless Channels,” *IEEE Transactions on Information Theory*, vol. 55, no. 7, pp. 3051–3073, July 2009.

[12] J. Dai, K. Niu, Z. Si, C. Dong, and J. Lin, “Polar–coded non–orthogonal multiple access,,” *IEEE Transactions on Signal Processing*, vol. 66, no. 5, pp. 1374–1389, March 2018.

[13] S. Jing, C. Yang, J. Yang, X. You, and C. Zhang, “Joint detection and decoding of polar–coded SCMA systems,” *2017 9th International Conference on Wireless Communications and Signal Processing (WCSP)*, pp. 1–6, 2017.

[14] X. Deng, J. Sha, X. Zhou, X. You, and C. Zhang, “Joint detection and decoding for polar–coded OFDM–IDMA systems,,” *2017 IEEE 12th International Conference on ASIC (ASICON)*, pp. 796–799, 2017.

[15] F. H. C. Novak and G. Matz, “Mimo-idma: Uplink multiuser mimo communications using interleavedivision multiple access and low-complexity iterative receivers,” *2007 IEEE International Conference on Acoustics, Speech and Signal Processing - ICASSP’07*, vol. 3, pp. III–225–III–228, 2007.

[16] R. Mori and T. Tanaka, “Performance of polar codes with the construction using density evolution,” *IEEE Communications Letters*, vol. 13, no. 7, pp. 519–521, July 2009.

[17] H. Saber and I. Marsland, “An incremental redundancy hybrid ARQ scheme via puncturing and extending of polar codes,,” *IEEE Transactions on Communications*, vol. 63, no. 11, pp. 3964–3973, November 2015.

[18] I. Tal and A. Vardy, “List decoding of polar codes,” *IEEE Transactions on Information Theory*, vol. 61, no. 5, pp. 2213–2226, May 2015.

[19] M. Chiu and W. Wu, “Reduced-complexity scl decoding of multi-crc-aided polar codes,” Sep 2016.

[20] H. Zhou, C. Zhang, W. Song, S. Xu, and X. You, “Segmented CRC–aided SC list polar decoding,” *2016 IEEE 83rd Vehicular Technology Conference (VTC Spring)*, pp. 1–5, 2016.

[21] B. Tomasi, F. Gabry, V. Bioglio, I. Land, and J. Belfiore, “Low–complexity receiver for multi–level polar coded modulationnon–orthogonal multiple access,,” *2017 IEEE Wireless Communications and Networking Conference Workshops (WCNCW)*, pp. 1–6, 2017.

[22] Z. Pan, E. Li, L. Wen, J. Lei, and C. Tang, “Joint iterative detection and decoding receiver for polar coded SCMA system,” *2018 IEEE International Conference on Communications Workshops (ICC Workshops)*, pp. 1–6, 2018.

[23] X. Wu and Z. Wu, “Performance analysis of SCMA system based on polar codes,” *2018 IEEE Globecom Workshops (GC Wkshps)*, pp. 1–5, 2018.

[24] P. Chaki and N. Kamiya, “A novel design of CRC–concatenated polar codes,,” *ICC 2019 - 2019 IEEE International Conference on Communications (ICC)*, pp. 1–6, 2019.